

# Northumbria Research Link

Citation: Eltouby, Pakinam, Shyha, Islam, Li, Chunchun and Khaliq, Jibran (2021) Factors Affecting the Piezoelectric Performance of Ceramic-Polymer Composites: A Comprehensive Review. *Ceramics International*, 47 (13). pp. 17813-17825. ISSN 0272-8842

Published by: Elsevier

URL: <https://doi.org/10.1016/j.ceramint.2021.03.126>  
<<https://doi.org/10.1016/j.ceramint.2021.03.126>>

This version was downloaded from Northumbria Research Link:  
<http://nrl.northumbria.ac.uk/id/eprint/45744/>

Northumbria University has developed Northumbria Research Link (NRL) to enable users to access the University's research output. Copyright © and moral rights for items on NRL are retained by the individual author(s) and/or other copyright owners. Single copies of full items can be reproduced, displayed or performed, and given to third parties in any format or medium for personal research or study, educational, or not-for-profit purposes without prior permission or charge, provided the authors, title and full bibliographic details are given, as well as a hyperlink and/or URL to the original metadata page. The content must not be changed in any way. Full items must not be sold commercially in any format or medium without formal permission of the copyright holder. The full policy is available online: <http://nrl.northumbria.ac.uk/policies.html>

This document may differ from the final, published version of the research and has been made available online in accordance with publisher policies. To read and/or cite from the published version of the research, please visit the publisher's website (a subscription may be required.)



**Northumbria  
University**  
NEWCASTLE



**University Library**

# **Factors Affecting Piezoelectric Performance of Ceramic-Polymer Composites: A Comprehensive Review**

Pakinam Eltouby<sup>a,b</sup>, Islam Shyha<sup>c</sup>, Chunchun Li<sup>d,e</sup> and Jibran Khaliq<sup>a\*</sup>,

<sup>a</sup>*Department of Mechanical and Construction Engineering, Faculty of Engineering and Environment, Northumbria University at Newcastle, NE1 8ST, UK*

<sup>b</sup>*Department of Industrial and Management Engineering, Arab Academy for Science, Technology and Maritime Transport, Abu Qir, PO Box 1029, Alexandria 21599, Egypt*

<sup>c</sup>*School of Engineering and The Built Environment, Edinburgh Napier University, Edinburgh EH10 5DT, UK*

<sup>d</sup>*College of Information Science and Engineering, Guilin University of Technology, Guilin, 541004, China*

<sup>e</sup>*School of Materials Science and Engineering, Nanchang University, Nanchang, 330031, China*

\* Corresponding Author: [\\*Jibran.khaliq@northumbria.ac.uk](mailto:*Jibran.khaliq@northumbria.ac.uk)

# **Factors Affecting the Piezoelectric Performance of Ceramic-Polymer Composites: A Comprehensive Review**

## **Abstract**

Over the past few decades, piezoelectric materials have emerged as one of the powerful platforms for energy harvesting applications. Nowadays, they offer sustainable solutions for high-performance, low-power electronic devices required in numerous industry fields such as aerospace, automotive, and biomedical devices. Ceramic-polymer piezoelectric composites combine the advantages of ceramics as well as the mechanical flexibility and weight of the polymers. This paper reviews various factors such as crystallinity, the orientation of filler particles, etc. that affect the piezoelectric performance. Generally, the piezoelectric performance can be measured using a variety of key parameters, such as piezoelectric charge coefficient ( $d_{33}$ ), piezoelectric voltage coefficient ( $g_{33}$ ), and dielectric constant ( $\epsilon_r$ ). The parameters are presented throughout the review to justify the enhancement of the piezoelectric performance of piezoceramic-polymer composites.

**Keywords:** Ceramic-polymer composites; dielectrics; piezoelectric materials; piezoelectric performance

## **1. Introduction**

Materials, whose characteristics such as shape [1] and colour [2] can be controlled by external stimuli, such as temperature, pressure, or an electric field, are referred as “smart materials”. The functional properties of such materials are multi-dimensional. They may include sensing and/or actuation capabilities [3] that may be reflected in actions such as self-sensing and self-repairing [4].

Among the vast array of available smart materials, the piezoelectric materials have been proven to have excellent potentials in various energy harvesting applications at a small scale, compared to solar and thermally based energy generators [5], [6,7]. Piezoelectric materials are those materials, capable of converting mechanical energy into electrical energy or vice versa [8].

Materials exhibiting piezoelectric properties are classified into three main categories, ceramics, polymers, and composites [9]. These materials can either exist naturally (such as quartz, cane sugar, collagen, topaz, and Rochelle salt) [6,10,11] or can be synthesised chemically such as perovskites [10,12], synthetic polymers [13–15] or piezoelectric composites [16,17]. These materials have characteristic individual advantages that can be beneficial towards specific applications. For instance, the porosity and hardness of ceramics may support tissue integration at the interface between tissue and a porous ceramic scaffold implant [18,19]. On the other hand, polymers offer mechanical flexibility over ceramics [20]; however, polymers do not offer the same electrical properties as ceramics do [21].

A composite material, on the other hand, integrates the desired traits of different materials (such as flexibility of polymer and electrical/mechanical properties of ceramics) to meet the stringent requirement for specific devices or applications efficiently. Most composites designs ensure strength and flexibility by reinforcing a relatively flexible but weaker polymer with a comparatively harder and stronger ceramic. Long-chain thermoplastic polymers generally exhibit a plastic behaviour and are ductile, easy to remould and recycle [22,23]. Recently, due to ease of processing, there has been an increased interest in enhancing the mechanical and electrical properties of thermoplastics as a matrix material for compositional material designs towards various applications [24–

26]. Moreover, there is a vast potential in the fabrication of low-cost, flexible, and efficient piezoelectric sensors by embedding piezoelectric active ceramic particles (as fillers) within a thermoplastic inactive polymer matrix. Numerous piezoelectric composites consisting of piezoelectric ceramics and piezoelectric polymers have been developed. There has been an increasing trend in the recent decade towards **the** fabrication of flexible piezoelectric materials which is evident by the increased number of **publications** in the area of piezoelectric composites as shown in Figure 1. Various compositions and advanced fabrication techniques such as dice and fill [18], injection moulding [19], lost mould [19], dielectrophoresis [27,28] and 3D printing [29] had been used to manufacture state of the art composites with an aim to reach properties comparable to ceramics. Each of these techniques has a distinctive impact on the piezoelectric performance of the fabricated composites, ranging from enhanced energy harvesting and energy storage capabilities [6,30], sensing applications [24,29,31,32] and tissue engineering [33]. However, fabrication techniques are not the only factor affecting the performance of the developed piezoelectric composites, therefore this review paper focuses on the investigation of the different factors affecting the performance of piezoelectric composites.

## 2. Parameters Governing Piezoelectricity

Piezoelectric materials are anisotropic with key indices that are necessary to measure performance.

### 2.1. Piezoelectric Charge or Strain Coefficient ( $d$ )

The piezoelectric charge coefficient,  $d_{ij}$  expresses the correlation between the generated electric charge for the applied mechanical stress, where the subscripts “i” and

“j” refer to the direction of the polarisation or charge motion and the direction of the mechanical stress, respectively [34]. A piezoelectric material could experience elongation or contraction depending on the relative direction of the applied electric field and the polarity of the material. Hence, the converse piezoelectric effect generates a strain that has a linear relationship to the applied electric field, and can be expressed in terms of tensor notation, thus (eq.1) [35]:

$$S_{jk} = d_{ijk} E_i \quad (1)$$

where  $S_{jk}$  is the piezoelectric strain,  $E_i$  is the applied electric field, and  $d_{ijk}$  is a third rank tensor of the piezoelectric coefficients.

Commonly, the piezoelectric coefficient used modes are longitudinal piezoelectric coefficient ( $d_{33}$ ), shear piezoelectric coefficient ( $d_{15}$ ), and transverse piezoelectric coefficient ( $d_{31}$ ) and ( $d_{24}$ ), that indicate the possible poling orientations and **force direction** [36]. The virgin piezoelectric body in form of either ceramics or single crystal has a randomly distributed polarization vector [37], which yields a macroscopic zero net polarization, and thus no piezoelectric properties. When applied a strong dc electric field, the electric dipoles are aligned with the direction of the electric field and remain after the dc field is removed (residual polarization). This process is called poling, after which the piezoelectric properties emerge [38].

The converse piezoelectric effect reflects the electric field-induced strain and has relevance towards actuator applications. As an index of domain wall motion, the piezoelectric strain coefficient ( $d_{ij}^*$ ) can be calculated through unipolar S-E (strain-electric field) curves ( $d_{ij}^* = [\text{pm/V}]$ ), using eq.2., where  $S_{\max}$  and  $E_{\max}$  represent maximum strength and maximum electric field, respectively [39]:

$$d_{ij} * = \frac{S_{max}}{E_{max}} \quad (2)$$

## 2.2. Permittivity

Permitivity of a dielectric material (oftened termed as dielectric permittivity and represented by symbol  $\epsilon$ ) may be defined by the electric displacement (D) and the applied electric field (E) at constant stress ( $\epsilon^T_{ij}$ ) or constant strain ( $\epsilon^S_{ij}$ ) where T and S represent stress and strain respectively (see eq.3). while the dielectric constant or relative permitivity ( $\epsilon_{r(ij)}$ ), which is the ability of a material to store energy is the ratio of the dielectric permittivity of a substance to the permittivity of free space as depicted by eq.4 [34].

$$\epsilon_{ij} = \frac{D_i}{E_j} \quad (3)$$

$$\epsilon_{r(ij)} = \frac{\epsilon_{ij}}{\epsilon_0} \quad (4)$$

## 2.3. Piezoelectric Voltage Coefficient (g)

The piezoelectric voltage coefficient is determined by the piezoelectric charge coefficient and the dielectric permittivity. The piezoelectric voltage coefficient is inversely proportional to the dielectric constant, and thus most piezoelectric materials usually consisting of inorganic ceramics with high dielectric constants, negatively impact their piezoelectric voltage coefficient values [40]. A ceramic-polymer composite on the other hand is a feasible option, where a high and measurable piezoelectric voltage constant can be achieved simply by mixing piezoelectric (ceramic) particles within a polymer matrix [41]. The value of  $g_{33}$  can be obtained using the formula in eq.5. [42]:

$$g_{33} = \frac{d_{33}}{\epsilon_0 \epsilon_r} \quad (5)$$

where  $\epsilon_0$  is the permittivity of free space taken as  $8.85 \times 10^{-12}$  F/m and  $\epsilon_r$  is the dielectric constant.

### **3. Piezoelectric Performance of Ceramic-Polymer Composites**

#### ***3.1. Overview of Piezoelectric Composites***

Although ceramics and polymers have their advantages and disadvantages which limit their uses and integration in various applications [11,43] their distinct advantages can be combined to create piezoelectric composites with better properties than their parent materials. Consequently, these piezoelectric composites can then provide the required mechanical integrity and flexibility from the polymer along with the piezoelectric properties offered by ceramics [36]. A general rule of thumb is, for a piezoelectric composite to exhibit electrical properties closer to ceramics, a higher volume fraction of filler needs to be added [44]. However, if a composite is manufactured having a desired distribution of fillers, the properties of composites can be further be tailored to suit the need of applications [45].

When fillers (ceramics) are mixed in a polymeric matrix to manufacture piezoelectric composites, the fillers can be categorised to having different “connectivity” between filler particles based on their arrangement inside the polymer matrix [46]. Connectivity in that context indicates the number of dimension coordinates (x, y, and z) a ceramic phase or a polymer phase is physically connected with itself. A phase denoted to the number 3, for instance, indicates the phase connection in all three dimensions. In the case of bi-phasic ceramic-polymer composites, a two-digit number system is used, where the first number

refers to the connectivity of the filler and the second number represents the connectivity of the matrix. There are ten patterns, illustrated in Figure 2, for ceramic and polymer phase connectivity with conformations ranging from a 0-0 unconnected pattern to a 3-3 pattern in which the ceramic and the polymer phases are three-dimensionally self-connected [46]. Amongst the vast array of connectivity possibilities, the 1-3 pattern has been extensively used in energy harvesting and biomedical applications such as ultrasound imaging, sensors, and hydroacoustic devices due to their high electromechanical coupling factor, hydrostatic voltage coefficient, and enhanced piezoelectric coefficient [47–50]. Another novelty in the 1-3 connectivity architectural configuration is the bio-inspired 1-3 piezoelectric composites emerging as promising candidates for flexible piezoelectric energy harvesting devices, due to their improved mechanical and piezoelectric properties when compared to conventional piezoelectric polymer composites with particle fillers [51].

There are at least four variant methods involved in the preparation of the 1-3 piezo composites including dice-and-fill [17], arrange-and-fill [17], injection moulding [19], and lost moulding [19] methods( see [Figure 3](#)). Connectivity via the first variant is achieved by cutting and subsequent backfilling and ultimately polishing of a sintered piezoelectric block [52]. As opposed to the dice-and-fill method, the arrange-and-fill method involves filling sintered ceramics within the polymer matrix before the cutting process. However, undesirable electromechanical responses could be triggered as a result of improper alignment of piezoceramic fillers, during fabrication processes like the arrange-and-fill [17]. Injection [moulding](#) is amongst the conventional methods available for the easy fabrication of composites. Using injection moulding, a ceramic green body with the typical rod-structure of 1-3 piezoceramic-polymer composites can be directly produced. After sintering, the parts run through the same procedure as the diced ceramic

block. However, the process is time-consuming, inflexible, and costly [53]. The lost mould method employs a technique that is accurate when compared to injection moulding. The process is initiated by using the LIGA (Lithography Galvano-forming and plastic moulding) process to manufacture a plastic mould **that** is filled with a slurry. Following drying, the mould is burned out and the structure is sintered to more than 98% of the X-ray density. However, the LIGA process is also **time-consuming and costly** [52].

### ***3.2. Factors Affecting the Piezoelectric Performance of Composites***

From the previous section of this article, it is evident that the enhanced performance of piezo composite-based devices highly depends not only on the fabrication process but also on the corresponding chemical and physical properties of the parent phases. This translates into the structural and functional property requirements of the individual phases that may bear on the composite, which includes requirements for the geometrical integrity of the composite. Therefore, it is of utmost importance to always determine the factors influencing the overall performance of piezo composites to streamline and guarantee effective material selection criteria that respond best to prime parameter indices during the fabrication process.

To date, several studies have investigated the development of various, chemical, and thermally stable energy storage devices [54–57]. The bulk of such devices could be manufactured using various fabrication methods such as dice-and-fill [58], 3D printing [55], and 4D printing [59] and at a reduced cost. However, this can only be feasible and sustainable when the factors determining performance **are** highly modulated to reflect targeted function(s). Insight from the literature suggests that factors affecting the piezoelectric performance may be categorised into at least six main factors and are represented in the Fish-bone diagram in Figure 4 and reviewed in the subsections below.

### *3.2.1. Temperature*

The selection of calcination temperature of piezoceramics and the determination of glass transitional temperature in **the** case of polymeric materials, intended for use as fillers and matrices in ceramic-polymer piezo composites are considered amongst the key factors, affecting the final electrical and dielectric performance of piezo composites [60,61]. This subsection reviews how the temperature, of either the intended embedded ceramic and/or polymer, significantly affects the final piezoelectric parameters. Several researchers have thus investigated the effect of the calcination temperature of the piezoceramic on the electrical properties of piezoelectric composites [62].

Perovskite piezoceramics could exist in different geometric phases so that they can be tuned through phase engineering to transit from one phase to another, to achieve enhanced piezoelectric properties [11]. There are three Morphotropic Phase Boundaries (MPB), representing the transitional composition phase [63] that could be exhibited by piezoceramics, viz: Rhombohedral-Tetrahedral (R-T), Orthorhombic-tetrahedral (O-T), and Rhombohedral-Orthorhombic (R-O) [64–67]. One of the common ways to enhance permittivity and piezoelectricity is to place materials at their phase transition boundaries [68].

Phase boundary is a temperature-dependent concept that greatly impacts the piezoelectricity of ceramics embedded in the polymer matrices. One of the options through which the morphotropic phase boundary (MPB) can be achieved is phase engineering, amongst which doping has been proven to effectively shift phase transition temperature exhibited by both lead-based [69] and lead-free piezoelectric materials [39]. In one such example, the MPB in the composition  $(K_{0.48}Na_{0.52})(NbO_3 - 0.05Ca_{0.2}(Bi_{0.5}Na_{0.5})0.8ZrO_3$  (KNN-CBNZ) was not achieved as the temperature

stability at the phase transition region (PTR) is critical in maintaining MPB. However, upon doping antimony, stable MPB was achieved which enhanced  $d_{33}$  from 300 pC/N to 470 pC/N [70]. Several other authors have also investigated the impact of chemical composition and reported enhanced piezoelectric properties due to MPB associated with the temperature stability in lead-free piezoceramic systems [71], [72] [73]. Figure 5 displays the impact of both the molar fraction composition during R-MPB-T transition and the impact of temperature during R-MPB-T transition on the  $d_{33}$  value in a 50Ba(Ti<sub>0.8</sub>Zr<sub>0.2</sub>)O<sub>3</sub>- 50(Ba<sub>0.7</sub>Ca<sub>0.3</sub>)TiO<sub>3</sub> (BZT-xBCT) ceramic. The maximum  $d_{33}$  value (620 pC/N) has been obtained at the MPB due to the facilitation of the polarisation rotation exhibited between the R-T phases [74]. Looking at the promising enhancement in the piezoelectric properties as a result of doping, doped piezoceramics are useful fillers in order to enhance the final piezoelectric properties of composites [75,76].

Despite the significant advances employed towards the enhancement of the piezo properties of ceramics, these strides can become relevant in piezo composites fabrications only when the designated polymeric matrix provides a suitable environment for the expression of the piezo properties. In polymers, the high degree of  $\pi$ - $\pi$  bond stacking in crystalline regions due to the regular atomic arrangement adopted by crystalline materials results in increased charge mobility in crystalline regions than in amorphous regions [77]. The semi-crystalline nature of most polymeric matrices used in composites has an impact on the efficiency of piezo active phases partly because such matrices exhibit higher viscosity than typical amorphous matrices [78]. This may influence the dipole alignment of the piezoceramic filler particles within a matrix such as Polylactic acid (PLA) because the working temperature is dependent on the melt viscosity [79,80]. Although polymers such as PLA generally require processing temperatures over 190-230°C [81,82], the glass-transition and melt temperature ( $T_m$ ) of their homopolymers is in the region of about 55°C

and 175 °C, respectively [79]. This poses a very narrow processing window that is generally improved by depressing the melting point via the addition of small amounts of lactide enantiomers of opposite configuration into the polymer. However, this strategy impacts negatively on crystallinity and the crystallisation rate [79].

Therefore, it is relevant to determine the glass transitional temperature ( $T_g$ ) of a polymeric material desired for use as the matrix in a piezo composite, because above the  $T_g$ , the composite acquires piezoelectric activity due to an efficient electric field caused by an increase in polymer matrix mobility and enhanced permittivity [83]. Additionally, temperature dynamics that impact the degradation of the polymeric matrix **have** a direct impact on the composite's piezoelectric properties. This is because a highly degraded matrix (a polymer of low crystallinity) may not provide the microstructural integrity required for alignment and stable activity of piezoceramic particles.

In 2015, Jing Fu et al. presented the impact of calcination temperature on the particle size and its effect on the dielectric properties of the composite. A molten salt synthesised BaTiO<sub>3</sub> (BT) single-crystalline nanostructures have been embedded in a modified barium titanate (PVP/BT)-PVDF composite. By employing various calcination temperatures, they used NaCl-KCL eutectic salts to develop different crystallite sizes of BT single-crystal nanoparticles (Figure 6). The results indicate that increases in particle size are a function of rising calcination temperature [84]. This phenomenon may be associated with the accelerated crystal growth occurring at high-temperature molten salt media [85]. In order to select the optimal particle size required for the composite preparation, the polarisation of the various particle sizes was determined [84]. Table 1 presents the temperature dependence of **the** dielectric constant for various volume fraction of **the** BT in a composite system. Generally, the dielectric constant of composites increases with an

increase in the volume fraction of the filler, while rising temperature enhances this trend. Within the investigated volume fractions, the dielectric constant increased consistently with increasing temperature for the different temperature regimes and increasing volume fraction, attending a peak at 60% volume fraction.

Furthermore, at 80% volume fraction, the dielectric constant attended a maximum at the maximum temperature of 130°C for the temperature range investigated. The enhanced dielectric constant is facilitated via spontaneous polarisation that is triggered as a function of increasing BT filler particle size for the peak fraction volume (which was 40% in for study) [84]. These findings may be partly associated with the filler particle size as well as the  $T_m$  (melt temperature) requirements of the polymer that necessitates the appropriate matrix environment influencing polarisation of the filler particles. In this way, the viscoelastic nature of matrix materials influences the electro-mechanical response of piezo composites [16]. Additionally, the calcination temperature employed for the piezoceramics may influence these findings via the crystal structure. Earlier investigations by several authors [86,87] have demonstrated the relationship between the spontaneous polarisation exhibited in BT particles and the tetragonality of the crystal (c/a). This relationship is presented in eq.6.

$$P_s \approx \left(\frac{c}{a}\right)^{0.5} \quad (6)$$

where  $P_s$  is the spontaneous polarisation.

Since tetragonality increases with increasing calcination temperature (from 650°C to 950°C) and c is directly proportional to polarisation ( $P_s$ ), the change exhibited in volume (atom displacement along with the perovskite structure) would hence enhance the piezoelectric properties. Despite the potential to enhance the average dielectric constant of composites, ceramic filler particles can generate inhomogeneous electric fields that

may weaken the polarisation response of the ceramic particles. This is due to ineffective breakdown strength and dispersion of electric field away from the piezo active particles [43,88]. However, surfactants and dispersants can be employed towards effective dispersion of piezo active filler particles [84], leading to improved interface compatibility.

### *3.2.2. Volume Fraction of the Filler*

One of the very significant factors affecting the overall performance of the dielectric properties of piezoelectric composites is the amount of ceramic volume fraction dispersed in the polymer matrix [89]. Therefore, in order to effectively assess the piezoelectric potential of a composite, the measurement of the filler volume fraction is employed as a vital tool in the morphological analysis of a piezoelectric composite. Volume fraction ( $V_f$ ) calculation is conducted based on the microscopic image from the specimen's cross-sections. By measuring the area of filler particle ( $A_f$ ) and a total area of **the** specimen's cross-section ( $A$ ), the filler volume fraction can be calculated using eq.7 [25]:

$$V_f = \frac{A_f}{A} \times 100 \quad (7)$$

where  $V_f$  is the volume fraction.

As discussed above, the dielectric constant is one of the key parameters to assess the piezoelectric performance of piezo composites. In the case of a composite composed of say a piezoceramic filler in a polymer matrix, the relationship governing the electric field ( $E_c$ ) acting on the ceramic particles and their dielectric constants, is given by eq.8. [30]:

$$E_c = \frac{3\epsilon_p}{\epsilon_c + 2\epsilon_p} E_0 \quad (8)$$

where  $\varepsilon_p$  and  $\varepsilon_c$  are the dielectric constants of the polymer and ceramic, respectively;  $E_0$  is the electric field applied to the composite. From the equation, it can be deduced that the electric field acting on the ceramic particles in a polymer matrix is controlled by the dielectric constant of the polymer matrix. Therefore, the efficiency of the piezoelectric ceramic poling can be achieved by enhancing the dielectric constant of the polymer [83]. Furthermore, the theoretical value for the dielectric constant ( $\varepsilon_r$ ) in the case of a piezoceramic filler in a polymer matrix composite has been predicted by Yamada et al. [90]. It can be obtained via the formula in eq.9:

$$\varepsilon_r = \varepsilon_p \left[ 1 + \frac{n\varphi(\varepsilon_c - \varepsilon_p)}{n\varepsilon_p + (1 - \varphi)(\varepsilon_c - \varepsilon_p)} \right] \quad (9)$$

where  $\varepsilon_p$  and  $\varepsilon_c$  are the dielectric constants of the polymer and the ceramic, respectively;  $n$  is the aspect ratio of the ceramic particles, and  $\varphi$  represents the ceramic filler volume fraction ( $= V_f$ ).

Jayendiran and Arockiarajan [91] have experimentally confirmed the theoretical modelling depicting the relationship between filler volume fraction and aspects such as remnant polarisation, saturation polarisation, and coercive electric field. The authors noted that in a 1-3 piezo composite of Lead Zirconium Titanate (PZT) fibres within an epoxy matrix, a decrease in fibre volume fraction resulted in a decrease in indices governing piezoelectricity that includes remnant polarisation and saturation polarisation (Table 2). The results indicate that both the remnant polarisation and the saturation polarisation have a direct relationship to the filler volume fraction. The mean values indicate that there is no significant discrepancy between experimental and theoretical values for both the remnant polarisation and saturation polarisation. The mean saturation polarisation of the composite increased significantly when 65% volume fraction PZT

fibres were used and marked when subsequent volume fractions (80% or 100%) were used. The effect of decreased filler volume fraction and consequent reduction in the number of dipoles is a decrease in the resistance to domain orientation provided by dipoles [92]. This notion has a direct significance to the dielectric permittivity and may be attributed to processing techniques [6,93] as well as the microstructure [93,94] of the material.

Frequency and temperature dependence are amongst the major outcomes of a piezo composite material composed of a piezo active particle of random distribution within the polymeric matrix. In 2017, Khan et al. reported the frequency and temperature dependence of the dielectric constant ( $\epsilon_r$ ) and loss tangent ( $\tan\delta$ ) for a piezoelectric composite composed of a random distribution of a Barium Titanate (BT) ceramic filler particles within a Thermoplastic Polyurethane (TPU) a matrix. The amount of electric energy lost in the form of heat by a material exposed to an external electric field is known as the dielectric loss ( $\tan \delta$ ). With increasing BT content within the composite, the  $\epsilon_r$ , and the  $\tan\delta$  increased, respectively, for each volume fraction of BT [95].

There seems to be a fair agreement between the experimental and the theoretical values of the reported  $\epsilon_r$ . The consistent rise in dielectric constant with the increasing volume fraction of the piezoelectric material imparts on the loss tangent with consequent enhancement of the electro-mechanical response of the material. However, increasing the volume fraction of BT may ultimately result in temperature and frequency dependence of the  $\epsilon_r$  and loss tangent [95]. Although there is not much discrepancy in the loss tangent reported across the various volume fractions, it is essential to note that there are other important factors that may account for the dielectric loss of a material, such as defects during polarisation hysteresis [19,85], dielectric leakages [19,84] nature of the external

environment and the technical process [39] that needs to be considered. Furtherly, in 2019, Kun Yu et al. [96] also investigated the impact of ceramic volume on the dielectric performance of a  $(K_{0.475}Na_{0.495}Li_{0.03})NbO_3$ -0.003ZrO<sub>2</sub> (KNNL-Z)/PVDF hot-pressed composite. The authors reported that the addition of KNNLZ-ceramic powder to the composite led to an increase in the dielectric permittivity. The observed improvement in dielectric permittivity is ascribed to the higher dielectric permittivity of KNN [97] compared to that of PVDF. This suggests that, although the filler volume fraction determines the dielectric properties of a composite, the specificity of the piezoceramic electro-mechanical capabilities is also directly vital in terms of dielectric enhancement.

The 1-3 composites have gained relevance due to their enhanced piezoelectric coefficient associated with their tailor-made useful properties and tunable acoustic impedance [98–100]. The relationships between the performance parameters of these composites and different ceramic volume fractions may be analysed via simulations and experimental measurements.

Recently Xu et al. [100] fabricated a three-phase material system of PZT-5A/epoxy resin/silicone rubber piezoelectric composites using the cutting-filling technique, with different piezoceramic volumes, having a 1-3 composite structure. The authors found an agreement between experimental and simulated results. They reported a linear relationship between both the dielectric constant and the piezoelectric coefficient ( $d_{33}$ ) of the composite and the piezoelectric volume fraction, indicating that the improved 1-3 piezoelectric composites are capable of exhibiting higher electromechanical coupling coefficients and electro-mechanical conversion efficiencies [100]. Both the  $d_{33}$  and the relative **permittivity** of the composites increase with an increase in the piezoceramic volume fraction. This trend is associated with the fact that PZT-5A has a relatively high  $d_{33}$  [101].

Moreover, Zhang et al., [102] investigated the piezoelectric and dielectric properties of lead-free porous  $0.5\text{Ba}(\text{Ca}_{0.8}\text{Zr}_{0.2})\text{O}_3\text{-}0.5(\text{Ba}_{0.7}\text{Ca}_{0.3})\text{TiO}_3$  (BCZT) ceramics. They reported that the porosity decreased the relative permittivity while a denser material increased the permittivity. Notably, increased porosity accounted for a significant drop in the  $d_{33}$  due to a drop in the remnant polarisation. The decrease in remnant polarisation may be associated with the fact that there is a concentration of the electric field in the low permittivity pore regions, during poling [103,104]. It is worthy to note that Siponkoski et al. has previously reported that the porous structure of a piezoelectric composite decreases the contact area between the matrix and the electrodes and causes a decrease in permittivity [105].

Composites possessing piezoelectric ceramic fillers with higher dielectric constants do not account for enhanced piezoelectric properties (**such as  $d_{33}$** ) because the fillers in such composites exhibit lower poling efficiency due to experiencing lower effective poling electric fields [106]. The graph in Figure 7 illustrates the dielectric constants versus the exhibited electric field calculated through four various PZT ceramics with different dielectric constants of piezoceramics. The effective electric field exhibited by the filler in the composite have been calculated using the formula in eq.10.:

$$E = \frac{(1 + R)\varepsilon_p}{\varepsilon_c + R\varepsilon_p} E_0 \quad (10)$$

where  $E$  is the effective exhibited electric poling field;  $R$  is the ratio of the average particle size to the inter-particle distance,  $\varepsilon_p$  and  $\varepsilon_c$  are the dielectric constants of the polymer and ceramic; respectively;  $E_0$  is the electric field applied to the composite. In all, the  $g_{33}$  of epoxy-PZ26 composites is higher than that of epoxy-PZ27, with a peak of  $\sim 79$  mV m/N at 10 vol%. These results were quite interesting as the general understanding for piezocomposites **was** to add ceramic filler with high  $d_{33}$  **to achieve highr  $d_{33}$  values**,

although, the determining factor was found to be dielectric constant rather than  $d_{33}$ . Similarly, for pyroelectric applications (as all piezoelectric materials are also pyroelectrics), low dielectric constant of the material inversely affect the pyroelectric Figure of Merit (FOM), which is the ability of a material to convert energy (thermal to electrical and vice versa) at a higher efficiency [107,108,109].

Moreover, Zhang et al., [104] have examined the influence of porosity on the polarisation-electric field behaviour of ferroelectric materials; they reported that higher porosity levels cause a significant reduction in an electric field and a rising level of the localised coercive field. Secondly, the various inclusion geometries of ceramic porosity were not considered [110]. An investigation of the geometries of various porous ceramics used as fillers in ceramic-polymer composite fabrication should be pursued, to establish the most efficient porous structure for a given application, in terms of piezoelectric coefficients. Therefore, biological and mechanical properties remain crucial in validating the piezoelectric performance of materials designated towards highly porous structural/functional applications such as is the case in bone tissue applications [111].

### *3.2.3. Crystallinity of Constituent Phases*

The microstructure of the constituent materials (ceramic and polymer) of a composite, is one of the factors that significantly influence the piezoelectric performance [112,113]. Therefore, it is essential to determine the degree of crystallinity in either case (ceramic and/or polymer), to achieve optimised piezoelectric performance [114].

It is always relevant to estimate the crystallinity for polymeric materials intended to use towards devices that require enhanced mechanical qualities such as good tensile strength and elasticity [77] because these properties are governed by the degree of crystallisation [78]. A high rate of crystallisation is a requirement for polymeric materials

used towards applications demanding high heat resistance [115] because the amorphous state is prone to rapid ageing (degradation) under ambient conditions.

In general, embedding single-crystal (SC) piezoelectric ceramic materials is preferred over polycrystalline piezoelectric materials [116], due to the higher piezoelectric charge coefficient exhibited by single-crystal ceramic materials [117]. Moreover, single-crystal piezoelectric materials have a higher performance than polycrystalline materials, in the coupling coefficient and the energy density. Therefore, the incorporation of the former in polymer-based piezoelectric composites has been intensively investigated. In 2000, T. Ritter investigated  $\text{Pb}(\text{Zn}_{1/3}\text{Nb}_{2/3})\text{O}_3$  (PZN) and  $\text{PbTiO}_3$  (PT) towards ultrasound transducer applications and effectively demonstrated that the incorporation of the single-crystal PZN-PT ceramic in their polymer-based composite resulted in an enhanced piezoelectric coefficient ( $d_{33}$  values) [118]. Recently, in 2018, Christopher Bowen et al. also investigated, among others, the dielectric properties and the piezoelectric voltage coefficient of a three-component SC/polymer/polymer composite having connectivity of 1-2-2. The composite was made of parallel piped-shaped SC rods (KNNTL:MN single - crystal) surrounded by a laminar polymer matrix which is composed of two polymers designated as Polymer I and Polymer II representing a volume fraction of the SC and Polymer I, respectively. Consequently, Polymer I represent a component with a larger stiffness and polymer II a smaller stiffness in the laminar matrix [47].

Although the superior piezoelectric and dielectric performance of single crystals than ceramics, the fragile properties are still a challenge to fabricate complex configurations using single-phase material. On the other hand, when used for the medical ultrasonic transducer, a drawback of piezoelectric single crystals is the relatively high acoustic impedance when compared to human tissue (1.5 MRayls). By incorporating single crystals with polymers matrix to form composites, the acoustic impedance, and

thickness electromechanical coupling factors can be tailored, leading to improved bandwidth and resolution of transducers. Therefore, intensive studies have been conducted on the incorporation of single crystals in polymer-based piezoelectric composites. Ritter et al. [118] reported a thickness coupling greater than 0.80 and widths of 75–141% were achieved in single-crystal PZN-8%PT 1-3 composite transducers. Oakley and Zipparo [119] reported on a 4 MHz 1–3 PZN–PT single crystal composite transducer with 100% –6 dB bandwidth and a 6 MHz PMN–PT transducer with 114% bandwidth. Lee et al. [120] reported a single-crystal/epoxy 1–3 composite with ternary  $\text{Pb}(\text{In}_{1/2}\text{Nb}_{1/2})\text{O}_3$ - $\text{Pb}(\text{Mg}_{1/3}\text{Nb}_{2/3})\text{O}_3$ - $\text{PbTiO}_3$  (PIN-PMN-PT) single crystal with  $d_{33}$  value on the order of  $\geq 960$  pC/N and a lower acoustic impedance (20 MRayl).

### *3.2.4. Alignment of Ceramic filler*

Several pieces of research have proven that aligning the ceramic particles in the polymer matrix eventually affects the dielectric properties of the piezoelectric composite. Recently, various attempts have been made during the particles alignment stage, in order to achieve enhanced properties [41,42,121].

Conventional manufacturing methods have employed dielectrophoresis (DEP) [26,27,122–124] as one of the techniques used for particles' alignment. During dielectrophoresis, the ceramic particles exhibit polarisation due to their exposure to a non-uniform/alternating electric field [27], upon which consequently the particles are aligned in a chain-like structure forming the so-called (structured) quasi 1-3 structure [125]. Figure 8 demonstrates a graphical representation of random 0-3, quasi 1-3, and conventional ceramic pillars 1-3 composite structure types along with their corresponding SEM images. Dielectrophoresis has been successfully used in the aligning of either

micron-sized cubes [41], fibres [126], or random spherical shaped particles [127] within the polymer matrix of a quasi 1-3 composite, with a resulting interparticle distance reduction and ultimately increasing the active phase within some areas of the composite. By increasing the piezoelectrically active phase and hence improving the particles connectivity, the  $d_{33}$  of an aligned quasi piezo composite exhibits a significant increase, compared to a composite having a random distribution of particles or 0-3 configuration. This is attributed to the correlation of the  $d_{33}$  value and the interparticle distance and particles' connectivity as described in the Van den Ende model [128]. Since the  $g_{33}$  is calculated by dividing the  $d_{33}$  over the relative permittivity of the composite, a significant enhancement in the  $g_{33}$  value is also exhibited.

Figure 9 illustrates the  $g_{33}$  of random 0-3 and dielectrophoretically aligned quasi 1-3 PZT-epoxy composites fabricated by Van den Ende at various PZT percentage volume fraction [129]. Generally, it can be deduced from Figure 9 that quasi 1-3 composites result in higher values of  $g_{33}$  at lower volume fraction achieving a maximum  $g_{33}$  value of 75 mVm/N at 10% PZT fraction in the polymer matrix, which is ascribed to the reduced interparticle distance and enhanced connectivity within the polymeric matrix.

Furthermore, recent studies by Daniella Deutz et al. indicate that composites composed of ceramic fibres filler in a polymeric matrix generate a greater enhancement of dielectric properties when compared to composites made of ceramic powder particles in a polymeric matrix. The authors fabricated a quasi 1-3 potassium sodium lithium niobate (KNLN) fibres-based composite towards energy harvesting applications using dielectrophoresis. They found out that in a piezoceramic-polymer composite, filler fibres have a greater capacity to improve dielectric properties than particle fillers counterparts. Herein, the dielectric enhancement potential exhibited by the fibres is attributed to the

reduced inter-particle distance exhibited by filler [126].

In recent years, research efforts towards enhancing the piezoelectric properties of composites have been partly achieved by altering the processing routes in the manufacturing of piezo composites. One of such strategies involves combining dielectrophoretic alignment and poling of quasi 1-3 composites at room temperature while the thermosetting polymer matrix is still in the liquid phase [130]. Earlier studies by Khanbareh et al. [131] have proven that the dielectric properties of piezo composites are affected by the electrical conductivity of the polymeric matrix. As with increased matrix' electrical conductivity, the build-up time of the electric field exhibited on the ceramic particles reduces, resulting in enhanced poling potential of the composites. Since, the electrical conductivity, as well as the permittivity of a thermosetting polymer such as epoxy, reduces upon curing, in 2017, Khanabareh et al. investigated the outcome of simultaneously carrying out DEP and the poling processes, while the polymer is in the liquid state, followed by subsequent curing. The authors reported a significant enhancement of the piezoelectric properties of the quasi 1-3 composites as a result of the simultaneous DEP and poling process[130]. This is ascribed to the enhanced poling efficiency of the composite and the improved formed chain-like structure.

In 2016, Kim et al. investigated the alignment of particles using the ice-templating technique [121]. Although the particles were aligned using a different method, the results indicated that the dielectric permittivity linearly increased with the BT fraction, confirming the dielectric permittivity as a function of the volume fraction of piezo active filler particles. One of the key aspects of the ice templating method is that the unique lamellar architecture achieved in the dielectric composite, affecting enhanced particle alignment in the composite, generates higher dielectric permittivities than conventionally

made composites. However, enhanced dielectric properties via the ice templating method are acquired at the upper threshold of the BT volume fraction (30%) (higher cost) as opposed to a lower BT volume fraction (10%) employed when using conventional dielectrophoretic alignment [106]. Secondly, although this method presents a promising platform for the enhancement of the dielectric properties and ultimate sensitivity of composites, the study did not consider the effect of the interface between piezo active particles and the matrix, which has been established using dielectrophoresis methods [26,41] as a key parameter governing piezoelectricity in composite materials. DEP alignment of piezo active particles within the polymeric matrix seems to be a preferred method in the fabrication of piezo composites targeting high sensitivities and cost-effectiveness.

### *3.2.5. Ternary Structures (Addition of a Third Phase)*

Conventional solid-state methods have been employed for the synthesis of piezoceramic ternary structures with improved piezoelectric properties such as enhanced piezoelectric coefficient ( $d_{33}$ ) and the Curie temperature ( $T_c$ ) [132]. The introduction of three-phase composites as a strategy towards the improvement of the piezoelectric properties of materials is becoming a significant area of scientific investigation [57].

In order to further enhance the dielectric properties of biphasic composites, several approaches based on including a third phase to the composite have been exploited [133], [134] such as the addition of conductive particles to the two-phase piezoelectric system [135]. Insight from literature highlighted that the addition of conductive carbon black particles to a PZT-PVDF composite resulted in an enhanced  $d_{33}$  of 42pC/N (at a composition of 0.7PZT/0.3PVDF and 0.4% carbon black) at 1kHz when compared to a  $d_{33}$  of 23pC/N for the same system but without carbon black inclusions [136]. The

addition of the conductive particles increases the conductivity of the composite, leading to enhanced polarisation properties that ultimately affect the dielectric properties. This illustrates that a three-phase composite of PZT/PVDF/Carbon black using carbon black as a modifier results in improved piezoelectric charge coefficients compared to the same system with no conductive particles.

Moreover, air (porosity) can also be introduced to reduce the dielectric constant of the polymeric matrix and subsequently enhance  $g_{33}$  [137]. The authors in this study, used thermal decomposition of polyurethane (PU) into its constituents to obtain the third phase, a gaseous phase. When di-isocyanate (component A) and polyol (component B) were reacted together, the hydrolysis of di-isocyanate resulted in the release of gas. Generally, given a model of a two-phase dielectric material, with gaseous content dispersed in a polymer matrix, in a serial mode of 0-3 composite with a homogeneous porosity within in the polymer matrix, there will be an exponential decrease in the dielectric constant of the air porosities as the gaseous content is increased. However, if a parallel mode of 1-3 exists, considering porosities as columns lengthened in the thickness direction, then the dielectric constant will decrease linearly when the gaseous content is increased [138]. Therefore, a two-phase porous polymer material with 0-3 modes is preferred because it provides a structural configuration with a decreased dielectric constant.

A composite made of BaTiO<sub>3</sub> and acrylonitrile butadiene styrene (ABS) may generate low permittivity due to poor particle/polymer interface bonding resulting from the porous nature of the inorganic additive. Additives such as organic esters have the potential of improving permittivity by enhancing the compatibility between polymer and filler ceramic particles in a composite [139]. Therefore, the employment of dispersants and surfactants [84] and plasticisers [22] may improve the fused deposition modelling (FDM)

printability of composites, due to their great potential to enhance dispersion of filler particles, and to decrease the viscosity of the composite, respectively.

### 3.2.6. *Electrical Conductivity of Constituents*

As mentioned in the introduction, piezoelectric materials have randomly distributed polarization vectors [37], and the application of a strong dc electric field would align the electric dipoles in a process called poling. Thus, the polymeric matrix should have certain electrical conductivity so the ceramic can be poled efficiently [140]. On the other hand, the polymer matrix should not be fully conductive. If electrical conductivity is higher than the percolation threshold of conducting filler, it will short circuit before poling finished. Very few papers have been reported which focus on enhancing electrical conductivity of either the matrix or of the filler in order to improve dielectric properties.

Recently, in 2018, Kim et al. investigated the effect of (FDM) on three-phase dielectric nanocomposites using poly(vinylidene) fluoride (PVDF), BaTiO<sub>3</sub>, and multiwall carbon nanotubes (CNTs) [141]. The authors incorporated CNT as a surfactant for BaTiO<sub>3</sub> as well as an electrically conductive filler and reported an enhancement in permittivity and dielectric constant that is associated with the improvement of BaTiO<sub>3</sub> dispersion and reduction in loss tangent, respectively.

## 4. Conclusions And Recommendations

In the ongoing quest to produce high-performance and cost-effective piezo ceramic-polymer composites fabrication methods capable of modulating the performance parameters is essential. Piezoelectric composites have the capacity to replace state-of-the-art ceramic materials in the application where integration is the key as they offer comparable piezoelectric sensing properties with an added benefit of flexibility.

With the global piezoelectric composites market predicted to reach nearly 400M USD, this review would aid in the manufacturing of piezoelectric composites with special emphasis of materials properties to improve piezoelectric performance. Much attention has been paid to improve piezoelectric properties of composites by altering the manufacturing techniques however, multiple other factors such as dielectric constant of the filler, addition of third phase and conductivity of the matrix also play a significant role in enhancing piezoelectric and dielectric properties of the composites. A keyway to improve piezoelectricity is to employ phase engineering options such as chemical composition modification and/or modulation of the sintering temperature, to place the materials at their phase transition region (PTR), where enhanced  $d_{33}$  and temperature stability can be achieved. Moreover, there has been scarcity of high performing flexible sensors at high temperature. High end polymers such as Polyetherimide (PEI), Polyimide (PI) could be used as passive matrices with a special focus on the dielectric properties of filler material and use of lead free materials such as KNN. In order to gain leverage across various industrial sectors, research efforts should include the investigation of parameters governing the thermal stability and degradability of piezoceramic-polymer composites. Bioabsorbable capacitor power sources are promising innovative options for piezo composite devices such as medical implants because of the potential to eliminate electronic waste and avoid unnecessary multiple surgeries.

## **5. Acknowledgement:**

Pakinam El-Touby would like to thank Northumbria University at Newcastle for providing the PhD funding to undertake the research work.

## References

- [1] K. Dai, C. Ning, Shape memory alloys and their medical applications, in: Biomech. Biomater. Orthop. Second Ed., Springer London, 2016: pp. 187–195.  
[https://doi.org/10.1007/978-1-84882-664-9\\_18](https://doi.org/10.1007/978-1-84882-664-9_18).
- [2] J. Zhang, J. Li, M. Huo, N. Li, J. Zhou, T. Li, J. Jiang, Photochromic Inorganic/Organic Thermoplastic Elastomers, *Macromol. Rapid Commun.* 38 (2017) 1–9. <https://doi.org/10.1002/marc.201700210>.
- [3] W.G. Drossel, H. Kunze, A. Bucht, L. Weisheit, K. Pagel, Smart3- Smart materials for smart applications, in: *Procedia CIRP*, 2015.  
<https://doi.org/10.1016/j.procir.2015.01.055>.
- [4] J. Mishra, Smart Materials-Types SS and Their Application: A Review, *Int. J. Mech. Prod. Eng.* (2017) 2321–2071.
- [5] X. Peng, T.W. Root, C.T. Maravelias, Storing solar energy with chemistry: The role of thermochemical storage in concentrating solar power, *Green Chem.* 19 (2017) 2427–2438. <https://doi.org/10.1039/c7gc00023e>.
- [6] N.A. Shepelin, A.M. Glushenkov, V.C. Lussini, P.J. Fox, G.W. Dicinoski, J.G. Shapter, A. V. Ellis, New developments in composites, copolymer technologies and processing techniques for flexible fluoropolymer piezoelectric generators for efficient energy harvesting, *Energy Environ. Sci.* 12 (2019) 1143–1176.  
<https://doi.org/10.1039/c8ee03006e>.
- [7] W. Poprawski, Z. Gnutek, J. Radojewski, R. Poprawski, Pyroelectric and dielectric energy conversion - A new view of the old problem, *Appl. Therm. Eng.* 90 (2015) 858–868. <https://doi.org/10.1016/j.applthermaleng.2015.07.031>.
- [8] B. Jaffe, W.R.C. Jr., H. Jaffe, *Piezoelectric Ceramics*, Academic Press Inc., 2012.
- [9] S. Mishra, L. Unnikrishnan, S.K. Nayak, S. Mohanty, Advances in Piezoelectric Polymer Composites for Energy Harvesting Applications: A Systematic Review, *Macromol. Mater. Eng.* 304 (2019) 1–25.  
<https://doi.org/10.1002/mame.201800463>.
- [10] E.A.R. Assirey, Perovskite synthesis, properties and their related biochemical and industrial application, *Saudi Pharm. J.* 27 (2019) 817–829.  
<https://doi.org/10.1016/j.jsp.2019.05.003>.

- [11] J. Hao, W. Li, J. Zhai, H. Chen, Progress in high-strain perovskite piezoelectric ceramics, *Mater. Sci. Eng. R Reports.* (2019).
- <https://doi.org/10.1016/j.mser.2018.08.001>.
- [12] R.H. Mitchell, M.D. Welch, A.R. Chakhmouradian, Nomenclature of the perovskite supergroup: A hierarchical system of classification based on crystal structure and composition, *Mineral. Mag.* 81 (2017) 411–461.
- <https://doi.org/10.1180/minmag.2016.080.156>.
- [13] X. Wang, F. Sun, G. Yin, Y. Wang, B. Liu, M. Dong, Tactile-sensing based on flexible PVDF nanofibers via electrospinning: A review, *Sensors (Switzerland)*. 18 (2018). <https://doi.org/10.3390/s18020330>.
- [14] L.S. Chafran, J.M.C. Campos, J.S. Santos, M.J.A. Sales, S.C.L. Dias, J.A. Dias, Synthesis of poly(lactic acid) by heterogeneous acid catalysis from d,l-lactic acid, *J. Polym. Res.* 23 (2016). <https://doi.org/10.1007/s10965-016-0976-7>.
- [15] Z. Li, J. Liao, Z. Xi, W. Zhu, Z. Zhang, Influence of Steric Hindrance on Ferro- and Piezoelectric Performance of Poly(vinylidene fluoride)-Based Ferroelectric Polymers, *Macromol. Chem. Phys.* 1900273 (2019) 1900273.
- <https://doi.org/10.1002/macp.201900273>.
- [16] R. Pramanik, A. Arockiarajan, A hybrid phenomenological model for thermo-mechano-electrical creep of 1–3 piezocomposites, *Philos. Mag.* 99 (2019) 1–21.
- <https://doi.org/10.1080/14786435.2018.1526417>.
- [17] R. Pramanik, A. Arockiarajan, Effective properties and nonlinearities in 1-3 piezocomposites: a comprehensive review, *Smart Mater. Struct.* 28 (2019) 103001. <https://doi.org/10.1088/1361-665x/ab350a>.
- [18] D. Zhou, K. Ho Lam, Y. Chen, Q. Zhang, Y. Ching Chiu, H. Luo, J. Dai, H. Lai Wa Chan, K.H. Lam, Y. Chen, Q. Zhang, Y.C. Chiu, H. Luo, J. Dai, H.L.W. Chan, Lead-free piezoelectric single crystal based 1–3 composites for ultrasonic transducer applications, *Sensors Actuators A Phys.* 182 (2012) 95–100.
- <https://doi.org/10.1016/j.sna.2012.05.030>.
- [19] H.J. Lee, S. Zhang, Y. Bar-Cohen, S. Sherrit, High Temperature, High Power Piezoelectric Composite Transducers, *Sensors (Switzerland)*. 14 (2014) 14526–14552. <https://doi.org/10.3390/s140814526>.

- [20] K. Uchino, Advanced Piezoelectric Materials: Science and Technology, Elsevier Science, 2017.
- [21] K.K. Sappati, S. Bhadra, Piezoelectric polymer and paper substrates: A review, Sensors (Switzerland). 18 (2018). <https://doi.org/10.3390/s18113605>.
- [22] S. Mahmud, Y. Long, M. Abu Taher, Z. Xiong, R. Zhang, J. Zhu, Toughening polylactide by direct blending of cellulose nanocrystals and epoxidized soybean oil, J. Appl. Polym. Sci. 48221 (2019) 1–13. <https://doi.org/10.1002/app.48221>.
- [23] C. Shuai, Y. Li, P. Feng, W. Yang, Z. Zhao, W. Liu, Montmorillonite reduces crystallinity of poly-l-lactic acid scaffolds to accelerate degradation, Polym. Adv. Technol. 30 (2019) 2425–2435. <https://doi.org/10.1002/pat.4690>.
- [24] J. Tolvanen, J. Hannu, J. Juuti, H. Jantunen, Piezoelectric Flexible LCP–PZT Composites for Sensor Applications at Elevated Temperatures, Electron. Mater. Lett. 14 (2018) 113–123. <https://doi.org/10.1007/s13391-018-0027-0>.
- [25] M. Heidari-Rarani, M. Rafiee-Afarani, A.M. Zahedi, Mechanical characterization of FDM 3D printing of continuous carbon fiber reinforced PLA composites, Compos. Part B Eng. 175 (2019) 107147.  
<https://doi.org/10.1016/j.compositesb.2019.107147>.
- [26] Khaliq, Hoeks, Groen, Fabrication of Piezoelectric Composites Using High-Temperature Dielectrophoresis, J. Manuf. Mater. Process. 3 (2019) 77.  
<https://doi.org/10.3390/jmmp3030077>.
- [27] H.A. Pohl, The Motion and Precipitation of Suspensoids in Divergent Electric Fields, J. Appl. Phys. 22 (1951) 869–871. <https://doi.org/10.1063/1.1700065>.
- [28] N. Kunnamkuzhakkal James, U. Lafont, S. van der Zwaag, W.A. Groen, Piezoelectric and mechanical properties of structured PZT-epoxy composites Daan van den Ende, (2012). <https://doi.org/10.1557/jmr.2012.428>.
- [29] H. Kim, F. Torres, D. Villagran, C. Stewart, Y. Lin, T.L.B. Tseng, 3D Printing of BaTiO<sub>3</sub>/PVDF Composites with Electric In Situ Poling for Pressure Sensor Applications, Macromol. Mater. Eng. 302 (2017) 1–6.  
<https://doi.org/10.1002/mame.201700229>.
- [30] F. Qi, N. Chen, Q. Wang, Dielectric and piezoelectric properties in selective laser sintered polyamide11/BaTiO<sub>3</sub>/CNT ternary nanocomposites, Mater. Des. 143

(2018) 72–80. <https://doi.org/10.1016/j.matdes.2018.01.050>.

- [31] C. Liu, N. Huang, F. Xu, J. Tong, Z. Chen, X. Gui, Y. Fu, C. Lao, 3D printing technologies for flexible tactile sensors toward wearable electronics and electronic skin, *Polymers (Basel)*. 10 (2018).  
<https://doi.org/10.3390/polym10060629>.
- [32] D. Yao, H. Cui, R. Hensleigh, P. Smith, S. Alford, D. Bernero, S. Bush, K. Mann, H.F. Wu, M. Chin-Nieh, G. Youmans, X. Zheng, Achieving the Upper Bound of Piezoelectric Response in Tunable, Wearable 3D Printed Nanocomposites, *Adv. Funct. Mater.* 29 (2019) 1903866.  
<https://doi.org/10.1002/adfm.201903866>.
- [33] T. Tariverdian, A. Behnamghader, P. Brouki Milan, H. Barzegar-Bafrooei, M. Mozafari, 3D-printed barium strontium titanate-based piezoelectric scaffolds for bone tissue engineering, *Ceram. Int.* 45 (2019) 14029–14038.  
<https://doi.org/10.1016/j.ceramint.2019.04.102>.
- [34] J. Holterman, P. Groen, An Introduction to Piezoelectric Materials and Applications, Stichting Applied Piezo, 2013.
- [35] G. Viola, T. Saunders, X. Wei, K.B. Chong, H. Luo, M.J. Reece, H. Yan, Contribution of piezoelectric effect, electrostriction and ferroelectric/ferroelastic switching to strain-electric field response of dielectrics, *J. Adv. Dielectr.* 03 (2013) 1350007. <https://doi.org/10.1142/s2010135x13500070>.
- [36] J.F. Tressler, S. Alkoy, R.E. Newnham, *Piezoelectric Sensors and Sensor Materials*, 1998.
- [37] D. Damjanovic, Piezoelectricity, in: *Encycl. Condens. Matter Phys.*, Elsevier, 2005: pp. 300–309. <https://doi.org/10.1016/B0-12-369401-9/00433-2>.
- [38] S. Fujishima, J. Merlini, J. Miyazaki, *Piezo Electric Ceramic Resonators and Filters.*, 1984. <https://doi.org/10.1109/freq.1984.200754>.
- [39] T. Zheng, J. Wu, D. Xiao, J. Zhu, Recent Development in Lead-Free Perovskite Piezoelectric Bulk Materials, *Prog. Mater. Sci.* 98 (2018) 552–624.  
<https://doi.org/10.1016/J.PMATSCI.2018.06.002>.
- [40] T.R. Shroud, S.J. Zhang, Lead-free Piezoelectric Ceramics: Alternatives for PZT?, *J. Electroceramics.* 19 (2007) 111–124. <https://doi.org/10.1007/s10832-007-9111-1>.

007-9047-0.

- [41] D.B. Deutz, N.T. Mascarenhas, J.B.J. Schelen, D.M. de Leeuw, S. van der Zwaag, P. Groen, Flexible Piezoelectric Touch Sensor by Alignment of Lead-Free Alkaline Niobate Microcubes in PDMS, *Adv. Funct. Mater.* 27 (2017) 1–7. <https://doi.org/10.1002/adfm.201700728>.
- [42] X. Gao, M. Zheng, X. Yan, J. Fu, M. Zhu, Y. Hou, The alignment of BCZT particles in PDMS boosts the sensitivity and cycling reliability of a flexible piezoelectric touch sensor, *J. Mater. Chem. C.* 7 (2019) 961–967. <https://doi.org/10.1039/c8tc04741c>.
- [43] Z.M. Dang, J.K. Yuan, S.H. Yao, R.J. Liao, Flexible nanodielectric materials with high permittivity for power energy storage, *Adv. Mater.* 25 (2013) 6334–6365. <https://doi.org/10.1002/adma.201301752>.
- [44] R. Li, H. Wang, P. Wang, H. Liu, J. Pei, Influence of PZT piezoelectric ceramics on the structure and electric properties of piezoelectric lead zirconate titanate/poly(vinylidene fluoride) composites, *Mater. Express.* 6 (2016) 483–492. <https://doi.org/10.1166/mex.2016.1336>.
- [45] R. Banks, R.L. O’Leary, G. Hayward, Enhancing the bandwidth of piezoelectric composite transducers for air-coupled non-destructive evaluation, *Ultrasonics*. 75 (2017) 132–144. <https://doi.org/10.1016/j.ultras.2016.10.007>.
- [46] L.. Newnham, R.E; Skinner, D.P; Cross, Connectivity and Piezoelectric-Pyroelectric Composite, *Mater. Res. Bull.* 13 (1978) 525–536. [https://doi.org/10.1016/0025-5408\(78\)90161-7](https://doi.org/10.1016/0025-5408(78)90161-7).
- [47] C.R. Bowen, V.Y. Topolov, Y. Zhang, A.A. Panich, 1-3-Type Composites Based on Ferroelectrics: Electromechanical Coupling, Figures of Merit, and Piezotechnical Energy-Harvesting Applications, *Energy Technol.* 6 (2018) 813–828. <https://doi.org/10.1002/ente.201700623>.
- [48] V.Y. Topolov, C.R. Bowen, A.N. Isaeva, Anisotropy factors and electromechanical coupling in lead-free 1-3-type composites, *IEEE Trans. Ultrason. Ferroelectr. Freq. Control.* 65 (2018) 1278–1286. <https://doi.org/10.1109/TUFFC.2018.2833856>.
- [49] R. Bao, M. Li, M. Shen, H. Liu, G. Zhang, Y. Zeng, S. Jiang, Enhanced

- pyroelectric properties of 1–3 nanocomposites achieved by uniaxial stretching, *J. Mater. Sci. Mater. Electron.* 30 (2019) 6760–6767.  
<https://doi.org/10.1007/s10854-019-00987-w>.
- [50] C. Zhou, J. Zhang, D. Liu, Z. Zhang, Novel 1–3 (K,Na)NbO<sub>3</sub>-based ceramic/epoxy composites with large thickness-mode electromechanical coupling coefficient and good temperature stability, *Ceram. Int.* 3 (2020) 7–11.  
<https://doi.org/10.1016/j.ceramint.2020.10.031>.
- [51] Y. Zhang, C.K. Jeong, T. Yang, H. Sun, L.Q. Chen, S. Zhang, W. Chen, Q. Wang, Bioinspired elastic piezoelectric composites for high-performance mechanical energy harvesting, *J. Mater. Chem. A* 6 (2018) 14546–14552.  
<https://doi.org/10.1039/c8ta03617a>.
- [52] A.A. Jain, P. K. J., A.K. Sharma, A.A. Jain, R. P.N, R.P.. Anjana Jain, Prashanth K. J., Asheesh Kr. Sharma, Arpit Jain, Dielectric and piezoelectric properties of PVDF/PZT composites: A review, *Polym. Eng. Sci.* 55 (2015) 1589–1616.  
<https://doi.org/10.1002/pen.24088>.
- [53] S. Schwarzer, A. Roosen, Tape casting of piezo ceramic/polymer composites, *J. Eur. Ceram. Soc.* 19 (1999) 1007–1010. [https://doi.org/10.1016/s0955-2219\(98\)00363-x](https://doi.org/10.1016/s0955-2219(98)00363-x).
- [54] H. Li, C. Zhao, X. Wang, J. Meng, Y. Zou, S. Noreen, L. Zhao, Z. Liu, H. Ouyang, P. Tan, M. Yu, Y. Fan, Z.L. Wang, Z. Li, Fully Bioabsorbable Capacitor as an Energy Storage Unit for Implantable Medical Electronics, *Adv. Sci.* 6 (2019) 1801625. <https://doi.org/10.1002/advs.201801625>.
- [55] Z. Wang, X. Yuan, J. Yang, Y. Huan, X. Gao, Z. Li, H. Wang, S. Dong, 3D-printed flexible, Ag-coated PNN-PZT ceramic-polymer grid-composite for electromechanical energy conversion, *Nano Energy*. 73 (2020) 104737.  
<https://doi.org/10.1016/j.nanoen.2020.104737>.
- [56] S. Kumar, S. Supriya, M. Kar, Enhancement of dielectric constant in polymer-ceramic nanocomposite for flexible electronics and energy storage applications, *Compos. Sci. Technol.* 157 (2018) 48–56.  
<https://doi.org/10.1016/j.compscitech.2018.01.025>.
- [57] A. Pal, A. Sasmal, B. Manoj, D.P. Rao, A.K. Haldar, S. Sen, Enhancement in

- energy storage and piezoelectric performance of three phase (PZT/MWCNT/PVDF) composite, Mater. Chem. Phys. 244 (2020) 122639. <https://doi.org/10.1016/j.matchemphys.2020.122639>.
- [58] F. Li, C. Chen, W. Li, D. Zeng, The electro-acoustic output behavior and thermal stability of 1–3 piezoelectric composite transducers applied to FUS surgery, J. Mater. Sci. Mater. Electron. 31 (2020) 12066–12073. <https://doi.org/10.1007/s10854-020-03735-7>.
- [59] D. Grinberg, S. Siddique, M. Le, R. Liang, J. Capsal, P. Cottinet, 4D Printing based piezoelectric composite for medical applications, J. Polym. Sci. Part B Polym. Phys. 57 (2019) 109–115. <https://doi.org/10.1002/polb.24763>.
- [60] K.M. Rittenmyer, Temperature dependence of the electromechanical properties of 0–3 PbTiO<sub>3</sub> -polymer piezoelectric composite materials, J. Acoust. Soc. Am. 96 (1994) 307–318. <https://doi.org/10.1121/1.410481>.
- [61] X. Kuang, Q. Gao, H. Zhu, Effect of calcination temperature of TiO<sub>2</sub> on the crystallinity and the permittivity of PVDF-TrFE/TiO<sub>2</sub> composites, J. Appl. Polym. Sci. 129 (2013) 296–300. <https://doi.org/10.1002/app.38729>.
- [62] R. Li, Z. Zhao, Z. Chen, J. Pei, Novel BaTiO<sub>3</sub>/PVDF composites with enhanced electrical properties modified by calcined BaTiO<sub>3</sub> ceramic powders, Mater. Express. 7 (2017). <https://doi.org/10.1166/mex.2017.1393>.
- [63] M. Ahart, M. Somayazulu, R.E. Cohen, P. Ganesh, P. Dera, H.K. Mao, R.J. Hemley, Y. Ren, P. Liermann, Z. Wu, Origin of morphotropic phase boundaries in ferroelectrics, Nature. 451 (2008) 545–548. <https://doi.org/10.1038/nature06459>.
- [64] Y. Huang, C. Zhao, X. Lv, H. Wang, J. Wu, Multiphase coexistence and enhanced electrical properties in (1-x-y)BaTiO<sub>3</sub>-xCaTiO<sub>3</sub>-yBaZrO<sub>3</sub> lead-free ceramics, Ceram. Int. 43 (2017) 13516–13523. <https://doi.org/10.1016/j.ceramint.2017.07.057>.
- [65] R. Sumang, C. Kornphom, T. Bongkarn, Synthesis and electrical properties of BNT-BKT-KNN lead free piezoelectric solid solution prepared via the combustion technique, Ferroelectrics. 518 (2017) 11–22. <https://doi.org/10.1080/00150193.2017.1360116>.

- [66] C. Li, L. Yang, J. Xu, C. Yuan, C. Zhou, H. Wang, The effect of artificial stress on structure, electrical and mechanical properties of Sr<sup>2+</sup> doped BNT–BT lead-free piezoceramics, *J. Mater. Sci. Mater. Electron.* 30 (2019) 21398–21405.  
<https://doi.org/10.1007/s10854-019-02518-z>.
- [67] D.A. Fernandez-Benavides, A.I. Gutierrez-Perez, A.M. Benitez-Castro, M.T. Ayala-Ayala, B. Moreno-Murguia, J. Muñoz-Saldaña, Comparative study of ferroelectric and piezoelectric properties of BNT-BKT-BT ceramics near the phase transition zone, *Materials (Basel)*. 11 (2018).  
<https://doi.org/10.3390/ma11030361>.
- [68] Y. Yao, C. Zhou, D. Lv, D. Wang, H. Wu, Y. Yang, X. Ren, Large piezoelectricity and dielectric permittivity in BaTiO<sub>3</sub>-xBaSnO<sub>3</sub> system: The role of phase coexisting, *EPL*. 98 (2012). <https://doi.org/10.1209/0295-5075/98/27008>.
- [69] Y. Feng, W.L. Li, D. Xu, W.P. Cao, Y. Yu, W.D. Fei, Enhanced piezoelectric properties and constricted hysteresis behaviour in PZT ceramics induced by Li<sup>+</sup>-Al<sup>3+</sup> ionic pairs, *RSC Adv.* 6 (2016) 36118–36124.  
<https://doi.org/10.1039/c6ra00152a>.
- [70] D. Pan, Y. Guo, X. Fu, R. Guo, H. Duan, Y. Chen, H. Li, H. Liu, Composition induced rhombohedral–tetragonal phase boundary and high piezoelectric activity in (K<sub>0.48</sub>,Na<sub>0.52</sub>) (Nb(1-x)Sbx)O<sub>3</sub> - 0.05Ca0.2(Bi0.5,Na0.5) 0.8ZrO<sub>3</sub> lead-free piezoelectric ceramics, *Solid State Commun.* 259 (2017) 29–33.  
<https://doi.org/10.1016/j.ssc.2017.05.001>.
- [71] D. Wang, A. Khesro, S. Murakami, A. Feteira, Q. Zhao, I.M. Reaney, Temperature dependent, large electromechanical strain in Nd-doped BiFeO<sub>3</sub>-BaTiO<sub>3</sub> lead-free ceramics, *J. Eur. Ceram. Soc.* 37 (2017) 1857–1860.  
<https://doi.org/10.1016/j.jeurceramsoc.2016.10.027>.
- [72] T. Zheng, H. Wu, Y. Yuan, X. Lv, Q. Li, T. Men, C. Zhao, D. Xiao, J. Wu, K. Wang, J.F. Li, Y. Gu, J. Zhu, S.J. Pennycook, The structural origin of enhanced piezoelectric performance and stability in lead free ceramics†, *Energy Environ. Sci.* 10 (2017) 528–537. <https://doi.org/10.1039/c6ee03597c>.
- [73] W. Bai, Y. Bian, J. Hao, B. Shen, J. Zhai, The composition and temperature-

- dependent structure evolution and large strain response in (1-x)(Bi 0.5 Na 0.5) TiO<sub>3</sub>-x Ba (Al 0.5 Ta 0.5) O<sub>3</sub> ceramics, *J. Am. Ceram. Soc.* 96 (2013) 246–252. <https://doi.org/10.1111/jace.12039>.
- [74] J. Gao, D. Xue, Y. Wang, D. Wang, L. Zhang, H. Wu, S. Guo, H. Bao, C. Zhou, W. Liu, S. Hou, G. Xiao, X. Ren, Microstructure basis for strong piezoelectricity in Pb-free Ba(Zr 0.2Ti0.8)O<sub>3</sub>-(Ba0.7Ca 0.3)TiO<sub>3</sub> ceramics, *Appl. Phys. Lett.* 99 (2011) 3–6. <https://doi.org/10.1063/1.3629784>.
- [75] K.H. Lam, H.L.W. Chan, Piezoelectric and pyroelectric properties of 65PMN-35PT/P(VDF-TrFE) 0-3 composites, *Compos. Sci. Technol.* 65 (2005) 1107–1111. <https://doi.org/10.1016/j.compscitech.2004.11.006>.
- [76] K.H. Lam, X. Wang, H.L.W. Chan, Piezoelectric and pyroelectric properties of (Bi0.5Na 0.5)0.94Ba0.06TiO<sub>3</sub>/P(VDF-TrFE) 0-3 composites, *Compos. Part A Appl. Sci. Manuf.* 36 (2005) 1595–1599. <https://doi.org/10.1016/j.compositesa.2005.03.007>.
- [77] S.Y. Son, Y. Kim, J. Lee, G.-Y. Lee, W.-T. Park, Y.-Y. Noh, C.E. Park, T. Park, High-Field-Effect Mobility of Low-Crystallinity Conjugated Polymers with Localized Aggregates, *J. Am. Chem. Soc.* 138 (2016) 8096–8103. <https://doi.org/10.1021/jacs.6b01046>.
- [78] S. Inkinen, M. Hakkarainen, A.-C. Albertsson, A. Södergård, From Lactic Acid to Poly(lactic acid) (PLA): Characterization and Analysis of PLA and Its Precursors, *Biomacromolecules*. 12 (2011) 523–532. <https://doi.org/10.1021/bm101302t>.
- [79] D. Garlotta, A Literature Review of Poly(Lactic Acid), 2001.
- [80] E. Castro-Aguirre, F. Iñiguez-Franco, H. Samsudin, X. Fang, R. Auras, Poly(lactic acid)—Mass production, processing, industrial applications, and end of life, *Adv. Drug Deliv. Rev.* 107 (2016) 333–366. <https://doi.org/10.1016/j.addr.2016.03.010>.
- [81] MAKERGEAR, PLA MSDS Sheet, PLA Filam. (2015).
- [82] SeeMeCNC, 3D PRINTER FILAMENT, SeeMeCNC 3D Printers More. (2018).
- [83] D. Carponcin, E. Dantras, L. Laffont, J. Dandurand, G. Aridon, F. Levallois, L. Cadiergues, C. Lacabanne, Integrated piezoelectric function in a high

- thermostable thermoplastic PZT/PEEK composite, *J. Non. Cryst. Solids.* 388 (2014) 32–36. <https://doi.org/10.1016/j.jnoncrysol.2014.01.020>.
- [84] J. Fu, Y. Hou, M. Zheng, Q. Wei, M. Zhu, H. Yan, Improving Dielectric Properties of PVDF Composites by Employing Surface Modified Strong Polarized BaTiO<sub>3</sub> Particles Derived by Molten Salt Method, *ACS Appl. Mater. Interfaces.* 7 (2015) 24480–24491. <https://doi.org/10.1021/acsami.5b05344>.
- [85] H. Ge, Y. Huang, Y. Hou, H. Xiao, M. Zhu, Size dependence of the polarization and dielectric properties of KNbO<sub>3</sub> nanoparticles, *RSC Adv.* 4 (2014) 23344–23350. <https://doi.org/10.1039/c4ra03613a>.
- [86] K. Xu, J. Li, X. Lv, J. Wu, X. Zhang, D. Xiao, J. Zhu, Superior Piezoelectric Properties in Potassium–Sodium Niobate Lead-Free Ceramics, *Adv. Mater.* 28 (2016) 8519–8523. <https://doi.org/10.1002/adma.201601859>.
- [87] W. Jo, R. Dittmer, M. Acosta, J. Zang, C. Groh, E. Sapper, K. Wang, J. Rödel, Giant electric-field-induced strains in lead-free ceramics for actuator applications - Status and perspective, *J. Electroceramics.* 29 (2012) 71–93. <https://doi.org/10.1007/s10832-012-9742-3>.
- [88] X. Wei, H. Yan, T. Wang, Q. Hu, G. Viola, S. Grasso, Q. Jiang, L. Jin, Z. Xu, M.J. Reece, Reverse boundary layer capacitor model in glass/ceramic composites for energy storage applications, *J. Appl. Phys.* 113 (2013) 024103. <https://doi.org/10.1063/1.4775493>.
- [89] P. Han, S. Pang, J. Fan, X. Shen, T. Pan, Highly enhanced piezoelectric properties of PLZT/PVDF composite by tailoring the ceramic Curie temperature, particle size and volume fraction, *Sensors Actuators, A Phys.* 204 (2013) 74–78. <https://doi.org/10.1016/j.sna.2013.10.011>.
- [90] T. Yamada, T. Ueda, T. Kitayama, Piezoelectricity of a high-content lead zirconate titanate/polymer composite, *J. Appl. Phys.* 53 (1982) 4328–4332. <https://doi.org/10.1063/1.331211>.
- [91] R. Jayendiran, A. Arockiarajan, Modeling of dielectric and piezoelectric response of 1-3 type piezocomposites, *J. Appl. Phys.* 112 (2012). <https://doi.org/10.1063/1.4748057>.
- [92] Chitra, A. Khandelwal, R. Gupta, R. Laishram, K.C. Singh, Impact of crystal

- structure and microstructure on electrical properties of Ho doped lead-free BCST piezoceramics, Ceram. Int. 45 (2019) 10371–10379.  
<https://doi.org/10.1016/j.ceramint.2019.02.095>.
- [93] D.B. Deutz, N.T. Mascarenhas, S. van der Zwaag, W.A. Groen, Enhancing energy harvesting potential of (K<sub>x</sub>Na<sub>1-x</sub>Li)NbO<sub>3</sub>-epoxy composites via Li substitution, J. Am. Ceram. Soc. 100 (2017) 1108–1117.  
<https://doi.org/10.1111/jace.14698>.
- [94] D.A. Van Den Ende, B.F. Bory, W.A. Groen, S. Van Der Zwaag, Improving the d<sub>33</sub> and g<sub>33</sub> properties of 0-3 piezoelectric composites by dielectrophoresis, J. Appl. Phys. 107 (2010) 0–8. <https://doi.org/10.1063/1.3291131>.
- [95] M.N. Khan, N. Jelani, C. Li, J. Khalil, Flexible and low cost lead free composites with high dielectric constant, Ceram. Int. 43 (2017) 3923–3926.  
<https://doi.org/10.1016/j.ceramint.2016.12.061>.
- [96] K. Yu, S. Hu, W. Yu, J. Tan, Piezoelectric and Dielectric Properties of ((K<sub>0.475</sub>Na<sub>0.495</sub>Li<sub>0.03</sub>)NbO<sub>3</sub>-0.003ZrO<sub>2</sub>)/PVDF Composites, J. Electron. Mater. 48 (2019) 2329–2337. <https://doi.org/10.1007/s11664-019-06978-1>.
- [97] S. Dwivedi, T. Pareek, S. Kumar, Structure, dielectric, and piezoelectric properties of K<sub>0.5</sub>Na<sub>0.5</sub>NbO<sub>3</sub>-based lead-free ceramics, RSC Adv. 8 (2018) 24286–24296. <https://doi.org/10.1039/c8ra04038a>.
- [98] C.R. Bowen, R. Stevens, L.J. Nelson, A.C. Dent, G. Dolman, B. Su, T.W. Button, M.G. Cain, M. Stewart, Manufacture and characterization of high activity piezoelectric fibres, Smart Mater. Struct. 15 (2006) 295–301.  
<https://doi.org/10.1088/0964-1726/15/2/008>.
- [99] W. Li-Kun, L. Li, Q. Lei, W. Weiwei, D. Tianxiao, Study of effective properties of modified 1-3 piezocomposites, J. Appl. Phys. 104 (2008).  
<https://doi.org/10.1063/1.2975343>.
- [100] J. Xu, L. Wang, C. Zhong, The effect of piezoceramic volume fraction on properties of three-phase piezocomposites, Ferroelectrics. 555 (2020) 132–145.  
<https://doi.org/10.1080/00150193.2019.1691391>.
- [101] R. Kiran, A. Kumar, R. Kumar, R. Vaish, Effect of poling orientation on piezoelectric materials operating in longitudinal mode, Mater. Res. Express. 6

(2019) 0–12. <https://doi.org/10.1088/2053-1591/ab0fd0>.

- [102] Y. Zhang, M. Xie, J. Roscow, C. Bowen, Dielectric and piezoelectric properties of porous lead-free 0.5Ba(Ca0.8Zr0.2)O<sub>3</sub>-0.5(Ba0.7Ca 0.3)TiO<sub>3</sub> ceramics, *Mater. Res. Bull.* 112 (2019) 426–431.  
<https://doi.org/10.1016/j.materresbull.2018.08.031>.
- [103] Y. Zhang, M. Xie, J. Roscow, Y. Bao, K. Zhou, D. Zhang, C.R. Bowen, Enhanced pyroelectric and piezoelectric properties of PZT with aligned porosity for energy harvesting applications, *J. Mater. Chem. A* 5 (2017) 6569–6580.  
<https://doi.org/10.1039/c7ta00967d>.
- [104] Y. Zhang, J. Roscow, R. Lewis, H. Khanbareh, V.Y. Topolov, M. Xie, C.R. Bowen, Understanding the effect of porosity on the polarisation-field response of ferroelectric materials, *Acta Mater.* 154 (2018) 100–112.  
<https://doi.org/10.1016/j.actamat.2018.05.007>.
- [105] T. Siponkoski, M. Nelo, J. Palosaari, J. Peräntie, M. Sobociński, J. Juuti, H. Jantunen, Electromechanical properties of PZT/P(VDF-TrFE) composite ink printed on a flexible organic substrate, *Compos. Part B Eng.* 80 (2015) 217–222.  
<https://doi.org/10.1016/j.compositesb.2015.05.018>.
- [106] J. Khalil, D.B. Deutz, J.A.C. Frescas, P. Vollenberg, T. Hoeks, S. van der Zwaag, P. Groen, Effect of the Piezoelectric Ceramic Filler Dielectric Constant on the Piezoelectric Properties of PZT-Epoxy Composites, *Ceram. Int.* 43 (2017) 2774–2779. <https://doi.org/10.1016/j.ceramint.2016.11.108>.
- [107] C.R. Bowen, J. Taylor, E. Leboulbar, D. Zabek, A. Chauhan, R. Vaish, Pyroelectric materials and devices for energy harvesting applications, *Energy Environ. Sci.* 7 (2014) 3836–3856. <https://doi.org/10.1039/c4ee01759e>.
- [108] B. Ploss, B. Ploss, F.G. Shin, A general formula for the effective pyroelectric coefficient of composites, *IEEE Trans. Dielectr. Electr. Insul.* 13 (2006) 1170–1176. <https://doi.org/10.1109/TDEI.2006.247846>.
- [109] C.R. Bowen, J. Taylor, E. Le Boulbar, D. Zabek, V.Y. Topolov, A modified figure of merit for pyroelectric energy harvesting, *Mater. Lett.* 138 (2015) 243–246. <https://doi.org/10.1016/j.matlet.2014.10.004>.
- [110] G. Martínez-Ayuso, M.I. Friswell, H. Haddad Khodaparast, J.I. Roscow, C.R.

- Bowen, Electric field distribution in porous piezoelectric materials during polarization, *Acta Mater.* 173 (2019) 332–341.  
<https://doi.org/10.1016/j.actamat.2019.04.021>.
- [111] S. Sadeghzade, R. Emadi, Improving the mechanical and bioactivity of hydroxyapatite porous scaffold ceramic with diopside/forstrite ceramic coating, *Nanomedicine J.* 6 (2019) 50–54. <https://doi.org/10.22038/nmj.2019.05.007>.
- [112] T. Lusiola, A. Soppelsa, F. Rubio-Marcos, J.F. Fernandez, F. Clemens, The impact of microstructure in (K,Na)NbO<sub>3</sub>-based lead-Free piezoelectric fibers: From processing to device production for structural health monitoring, *J. Eur. Ceram. Soc.* 36 (2016) 2745–2754.  
<https://doi.org/10.1016/j.jeurceramsoc.2016.04.009>.
- [113] H.G. Lee, H.G. Kim, Influence of Microstructure on the Dielectric and Piezoelectric Properties of Lead Zirconate-Polymer Composites, *J. Am. Ceram. Soc.* 72 (1989) 938–942. <https://doi.org/10.1111/j.1151-2916.1989.tb06248.x>.
- [114] L. Zhang, X. Shan, P. Bass, Y. Tong, T.D. Rolin, C.W. Hill, J.C. Brewer, D.S. Tucker, Z.Y. Cheng, Process and Microstructure to Achieve Ultra-high Dielectric Constant in Ceramic-Polymer Composites, *Sci. Rep.* 6 (2016) 1–10.  
<https://doi.org/10.1038/srep35763>.
- [115] R. Zhang, Y. Wang, K. Wang, G. Zheng, Q. Li, C. Shen, Crystallization of poly(lactic acid) accelerated by cyclodextrin complex as nucleating agent, *Polym. Bull.* 70 (2013) 195–206. <https://doi.org/10.1007/s00289-012-0814-y>.
- [116] D. Maurya, Y. Yan, S. Priya, Piezoelectric materials for energy harvesting, *Adv. Mater. Clean Energy.* (2015) 143–178. <https://doi.org/10.1201/b18287>.
- [117] S. Zhang, F. Li, J. Luo, R. Sahul, T. Shrout, Relaxor-PbTiO<sub>3</sub> single crystals for various applications, *IEEE Trans. Ultrason. Ferroelectr. Freq. Control.* 60 (2013) 1573–1579. <https://doi.org/10.1109/TUFFC.2013.2737>.
- [118] T. Ritter, Single crystal pzn-pt-polymer composites for ultrasound transducer applications, *IEEE Trans. Ultrason. Ferroelectr. Freq. Control.* 47 (2000) 792–800. <https://doi.org/10.1109/58.852060>.
- [119] C.G. Oakley, M.J. Zippardo, Single crystal piezoelectrics: A revolutionary development for transducers, *Proc. IEEE Ultrason. Symp.* 2 (2000) 1157–1167.

<https://doi.org/10.1109/ultsym.2000.921530>.

- [120] H.J. Lee, S. Zhang, T.R. Shrout, Scaling effects of relaxor-PbTiO<sub>3</sub> crystals and composites for high frequency ultrasound, *J. Appl. Phys.* 107 (2010).
- <https://doi.org/10.1063/1.3437068>.
- [121] D.S. Kim, C. Baek, H.J. Ma, D.K. Kim, Enhanced dielectric permittivity of BaTiO<sub>3</sub>/epoxy resin composites by particle alignment, *Ceram. Int.* 42 (2016) 7141–7147. <https://doi.org/10.1016/j.ceramint.2016.01.103>.
- [122] D.A. Van Den Ende, B.F. Bory, W.A. Groen, S. Van Der Zwaag, Improving the d<sub>33</sub> and g<sub>33</sub> properties of 0-3 piezoelectric composites by dielectrophoresis, *J. Appl. Phys.* 107 (2010) 24107. <https://doi.org/10.1063/1.3291131>.
- [123] H. Khanbareh, S. van der Zwaag, W.A. Groen, In-situ poling and structurization of piezoelectric particulate composites, *J. Intell. Mater. Syst. Struct.* 28 (2017) 2467–2472. <https://doi.org/10.1177/1045389X17689928>.
- [124] H. Khanbareh, S. Van Der Zwaag, W.A. Groen, Effect of dielectrophoretic structuring on piezoelectric and pyroelectric properties of lead titanate-epoxy composites, *Smart Mater. Struct.* 23 (2014). <https://doi.org/10.1088/0964-1726/23/10/105030>.
- [125] A. Mittal, Three Phase Piezoelectric Composites for Energy Harvesting Application, Delft, 2018.
- [126] V. Stuber, D. Deutz, J. Bennett, D. Cannell, D. de Leeuw, S. van der Zwaag, P. Groen, Flexible lead-free Piezoelectric Composite Materials for Energy Harvesting Applications, *Energy Technol.* 6 (2018) 1–10.  
<https://doi.org/10.1002/ente.201800419>.
- [127] S.A. Wilson, G.M. Maistros, R.W. Whatmore, Structure modification of 0-3 piezoelectric ceramic/polymer composites through dielectrophoresis, *J. Phys. D. Appl. Phys.* 38 (2005) 175–182.
- [128] D.A. Van Den Ende, S.E. Van Kempen, X. Wu, W.A. Groen, C.A. Randall, S. Van Der Zwaag, Dielectrophoretically structured piezoelectric composites with high aspect ratio piezoelectric particles inclusions, *J. Appl. Phys.* 111 (2012) 124107. <https://doi.org/10.1063/1.4729814>.
- [129] D.A. Van den Ende, Structured Piezoelectric Composites, University of Delft,

2012.

- [130] H. Khanbareh, S. van der Zwaag, W. Groen, In-situ poling and structurization of piezoelectric particulate composites, *J. Intell. Mater. Syst. Struct.* 28 (2017) 2467–2472. <https://doi.org/10.1177/1045389X17689928>.
- [131] H. Khanbareh, S. Van Der Zwaag, W.A. Groen, Piezoelectric and pyroelectric properties of conductive polyethylene oxide-lead titanate composites, *Smart Mater. Struct.* 24 (2015). <https://doi.org/10.1088/0964-1726/24/4/045020>.
- [132] T.L. Zhao, C. Fei, X. Dai, J. Song, S. Dong, Structure and enhanced piezoelectric performance of BiScO<sub>3</sub>-PbTiO<sub>3</sub>-Pb(Ni<sub>1/3</sub>Nb<sub>2/3</sub>)O<sub>3</sub> ternary high temperature piezoelectric ceramics, *J. Alloys Compd.* 806 (2019) 11–18. <https://doi.org/10.1016/j.jallcom.2019.07.286>.
- [133] S. George, M.T. Sebastian, Three-phase polymer-ceramic-metal composite for embedded capacitor applications, *Compos. Sci. Technol.* 69 (2009) 1298–1302. <https://doi.org/10.1016/j.compscitech.2009.03.003>.
- [134] W. Li, Z. Song, J. Qian, H. Chu, X. Wu, Z. Tan, W. Nie, Surface modification-based three-phase nanocomposites with low percolation threshold for optimized dielectric constant and loss, *Ceram. Int.* 44 (2018) 4835–4844. <https://doi.org/10.1016/j.ceramint.2017.12.072>.
- [135] W. Tuff, P. Manghera, J. Tilghman, E. Van Fossen, S. Chowdhury, S. Ahmed, S. Banerjee, BaTiO<sub>3</sub>–Epoxy–ZnO-Based Multifunctional Composites: Variation in Electron Transport Properties due to the Interaction of ZnO Nanoparticles with the Composite Microstructure, *J. Electron. Mater.* 48 (2019) 4987–4996. <https://doi.org/10.1007/s11664-019-07292-6>.
- [136] R. Li, Q. Guo, Z. Shi, J. Pei, Effects of conductive carbon black on PZT/PVDF composites, *Ferroelectrics.* 526 (2018) 176–186. <https://doi.org/10.1080/00150193.2018.1456308>.
- [137] H. Khanbareh, K. de Boom, S. van der Zwaag, W.A. Groen, Highly sensitive piezo particulate-polymer foam composites for robotic skin application, *Ferroelectrics.* 515 (2017) 25–33. <https://doi.org/10.1080/00150193.2017.1360101>.
- [138] N. Chand, J. Sharma, Influence of porosity on resistivity of polypropylene foams,

- (n.d.). <https://doi.org/10.1177/0021955X11427190>.
- [139] I. Cooperstein, E. Sachyani-Keneth, E. Shukrun-Farrell, T. Rosental, X. Wang, A. Kamyshny, S. Magdassi, Hybrid Materials for Functional 3D Printing, *Adv. Mater. Interfaces*. 5 (2018). <https://doi.org/10.1002/admi.201800996>.
- [140] C.K. Wong, F.G. Shin, Effect of electrical conductivity on poling and the dielectric, pyroelectric and piezoelectric properties of ferroelectric 0-3 composites, *J. Mater. Sci.* 41 (2006) 229–249. <https://doi.org/10.1007/s10853-005-7243-3>.
- [141] H. Kim, J. Johnson, L.A. Chavez, C.A. Garcia Rosales, T.L.B. Tseng, Y. Lin, Enhanced dielectric properties of three phase dielectric MWCNTs/BaTiO<sub>3</sub>/PVDF nanocomposites for energy storage using fused deposition modeling 3D printing, *Ceram. Int.* 44 (2018) 9037–9044. <https://doi.org/10.1016/j.ceramint.2018.02.107>.
- [142] J.A. Gallego-Juarez, Piezoelectric Ceramics and Ultrasonic Transducers, *J. Phys. E Sci. Instrum.* 22 (1989) 804–816.

## List of Figures

Figure 1: Number of publications on piezoelectric composites (data taken from web of science and correct as of November 2020).....	45
Figure 2. Different types of connectivity of the two-phase composite system [140]....	46
Figure 3. Schematics of 1-3 piezocomposites fabrication: (A) dice-and-fill; (B) arrange-and-fill; (C) injection moulding techniques from [19]. .....	47
Figure 4. Fishbone diagram of various factors affecting the piezoelectric performance of a piezoelectric composite.....	48
Figure 5. (a) Ba(Ti <sub>0.8</sub> Zr <sub>0.2</sub> )O <sub>3</sub> - x(Ba <sub>0.7</sub> Ca <sub>0.3</sub> )TiO <sub>3</sub> ceramic phase diagram near the MPB; (b) composition-dependence of d <sub>33</sub> during composition-induced R-MPB-T transition along the red horizontal line displayed in (a); (c) temperature-dependence of d <sub>33</sub> during temperature-induced R-MPB-T transition along the blue vertical line displayed in (a); from [74].....	49
Figure 6. SEM micrographs of BT different-sized particles calcined at various temperatures in degree Celsius (a) 600 (b) 650 (c) 750 (d) 850 (e) 950 (f) 1000 from [84] .....	50
Figure 7. The effect of dielectric constant of the filler on the effective electric field (poled at 10kV/mm)(Data taken from [106] and [41]).....	51
Figure 8. Graphical representation of 0-3, quasi 1-3 and conventional ceramic pillars 1-3 composite types along with their corresponding SEM micrographs; in random and quasi composite, the polymer matrix is white whilst ceramic filler is grey coloured from [34] and [106].....	52
Figure 9. g <sub>33</sub> of random 0-3 and structured 1-3 PZT/polymer composite at various PZT volume fraction adopted from [127].....	53

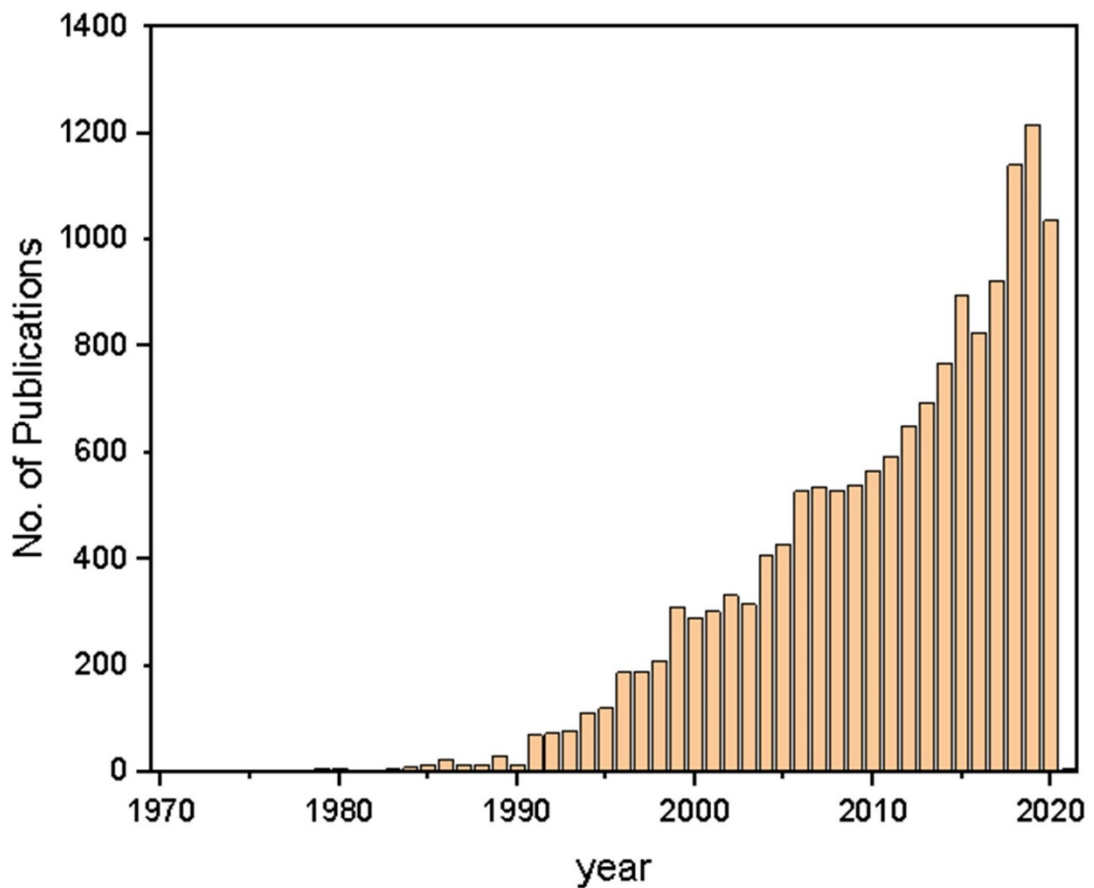


Figure 1: Number of publications on piezoelectric composites (data taken from web of science and correct as of November 2020)

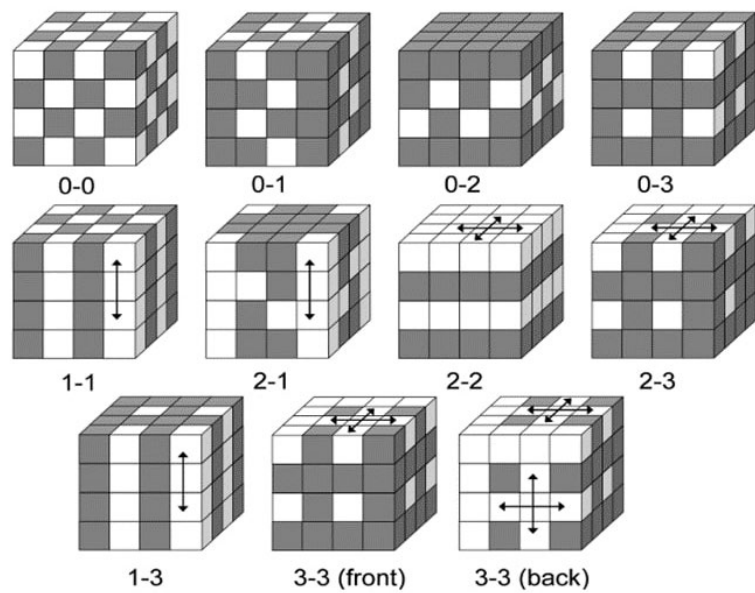


Figure 2. Different types of connectivity of the two-phase composite system [142]

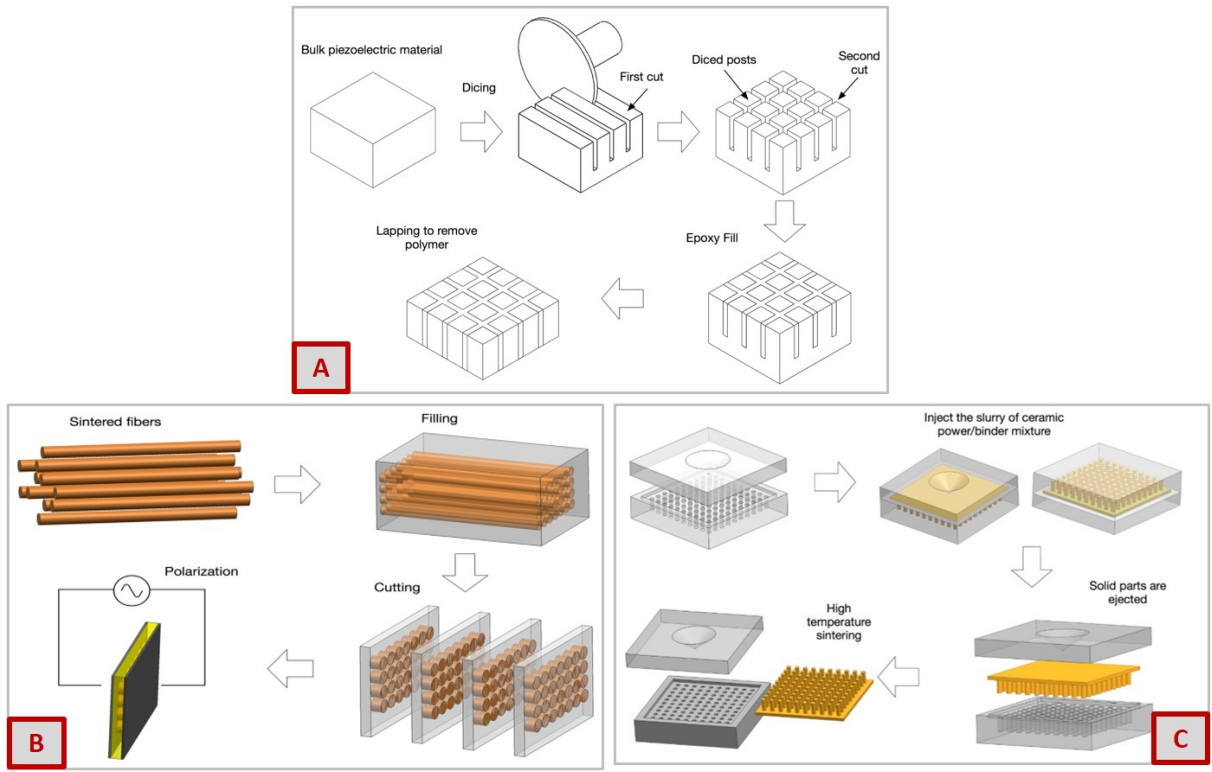


Figure 3. Schematics of 1-3 piezocomposites fabrication: (A) dice-and-fill; (B) arrange-and-fill; (C) injection moulding techniques from [19].

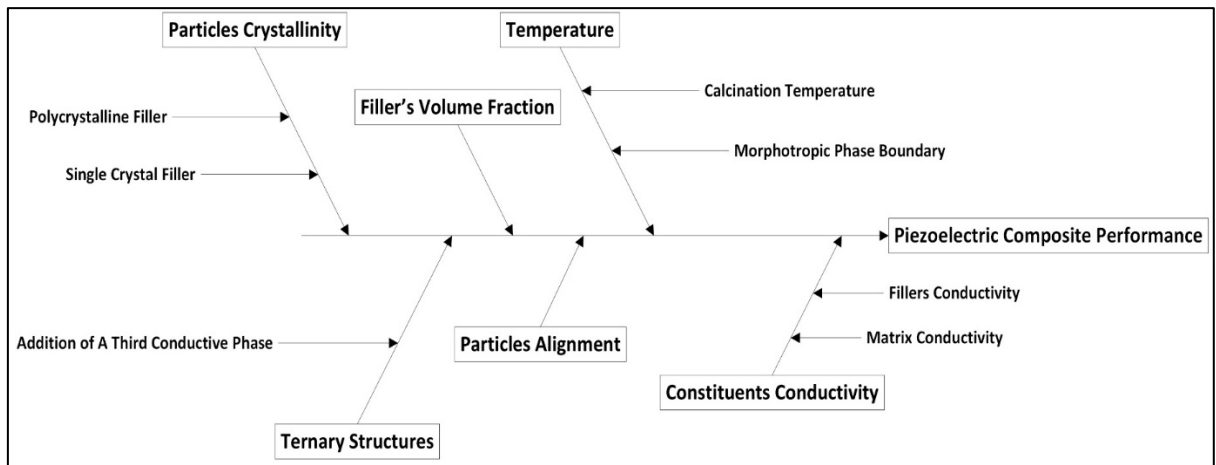


Figure 4. Fishbone diagram of various factors affecting the piezoelectric performance of a piezoelectric composite

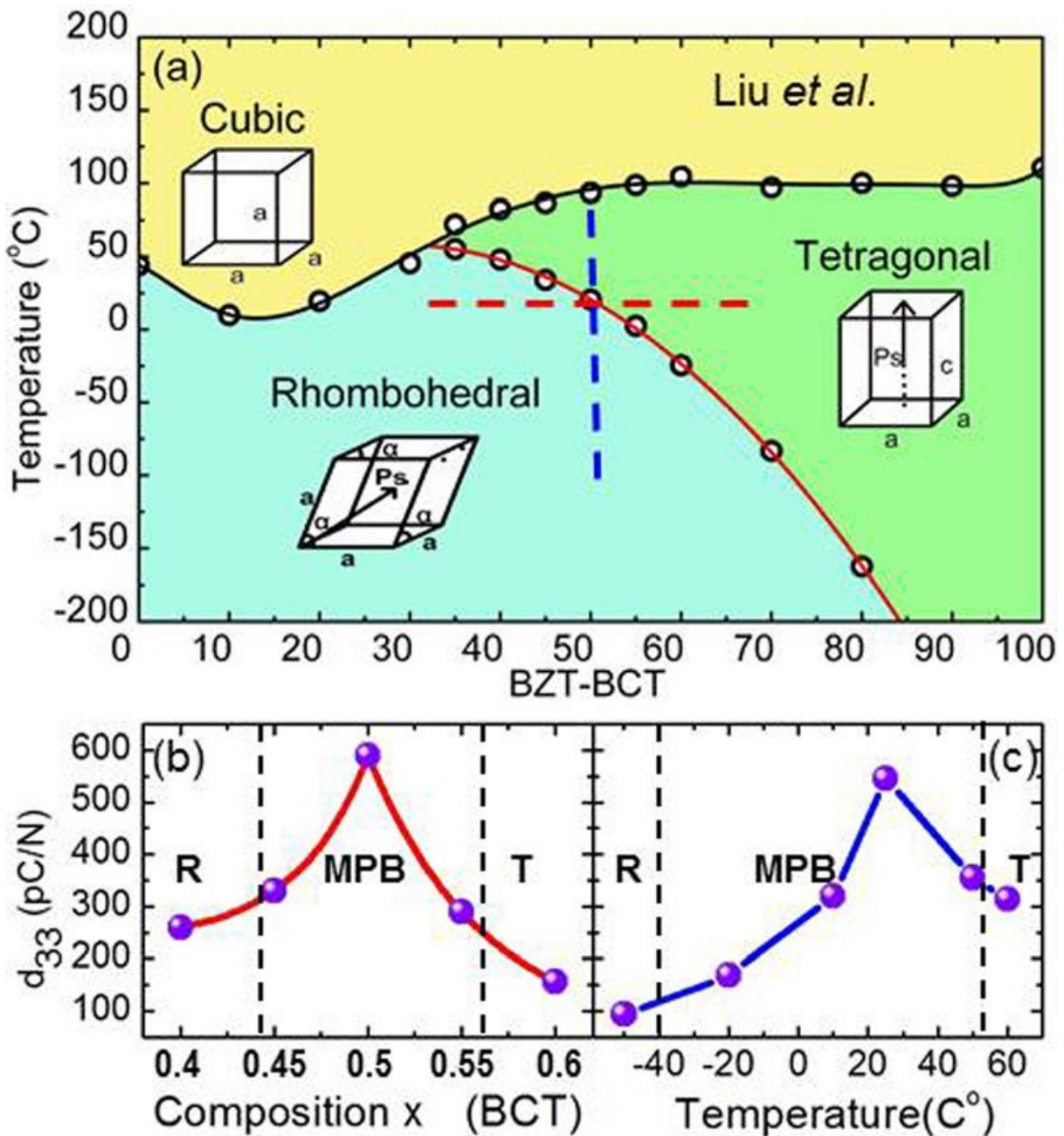


Figure 5. (a)  $\text{Ba}(\text{Ti}_{0.8}\text{Zr}_{0.2})\text{O}_3$ - $x(\text{Ba}_{0.7}\text{Ca}_{0.3})\text{TiO}_3$  ceramic phase diagram near the MPB; (b) composition-dependence of  $d_{33}$  during composition-induced R-MPB-T transition along the red horizontal line displayed in (a); (c) temperature-dependence of  $d_{33}$  during temperature-induced R-MPB-T transition along the blue vertical line displayed in (a);

from [74]

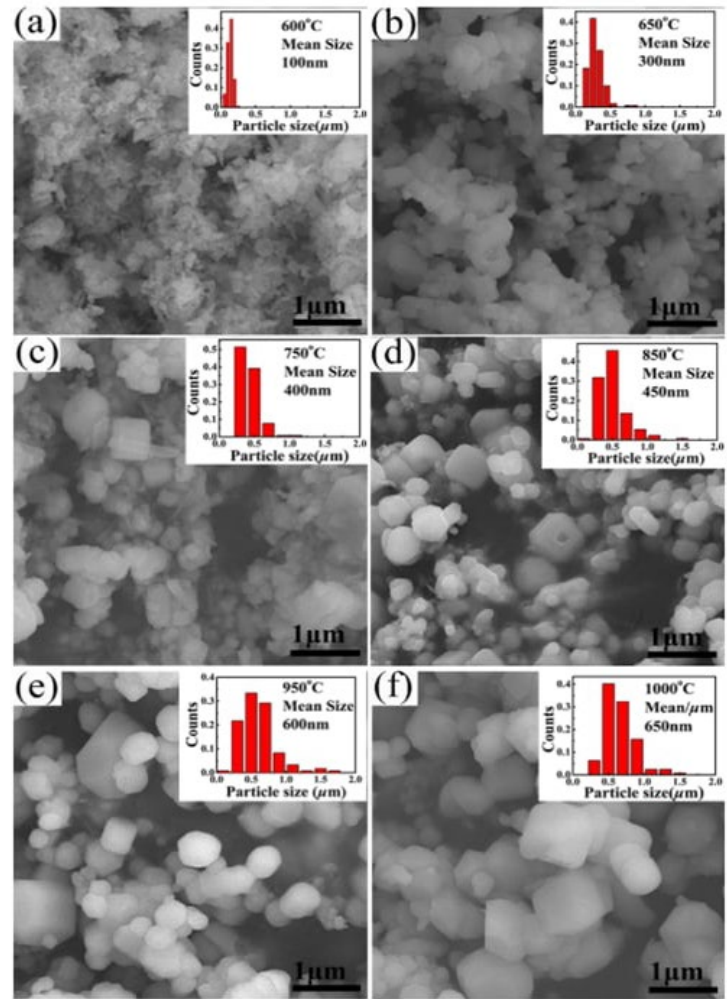


Figure 6. SEM micrographs of BT different-sized particles calcined at various temperatures in degree Celsius (a) 600 (b) 650 (c) 750 (d) 850 (e) 950 (f) 1000 from [84]

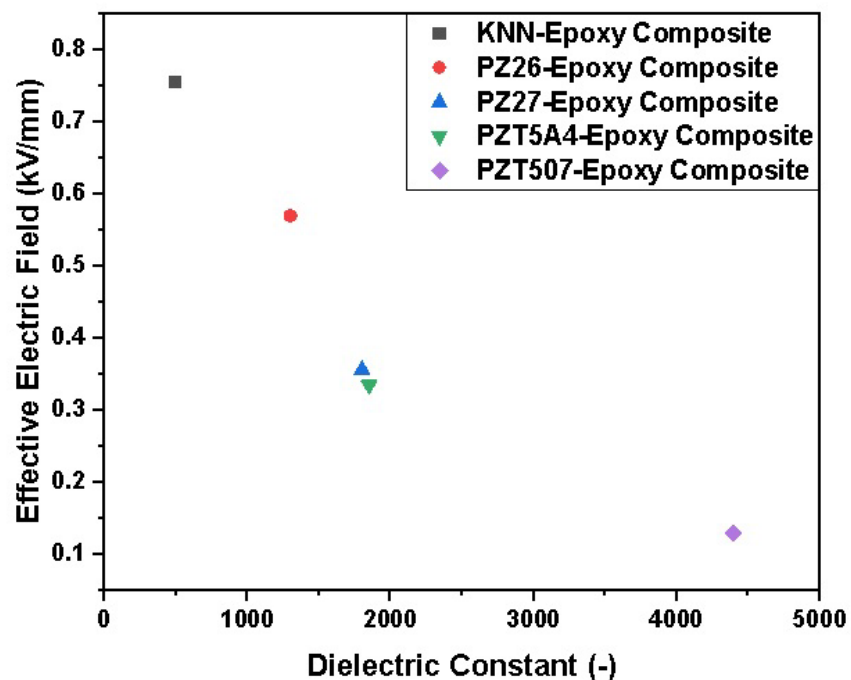


Figure 7. The effect of dielectric constant of the filler on the effective electric field  
(poled at 10kV/mm)(Data taken from [106] and [41])

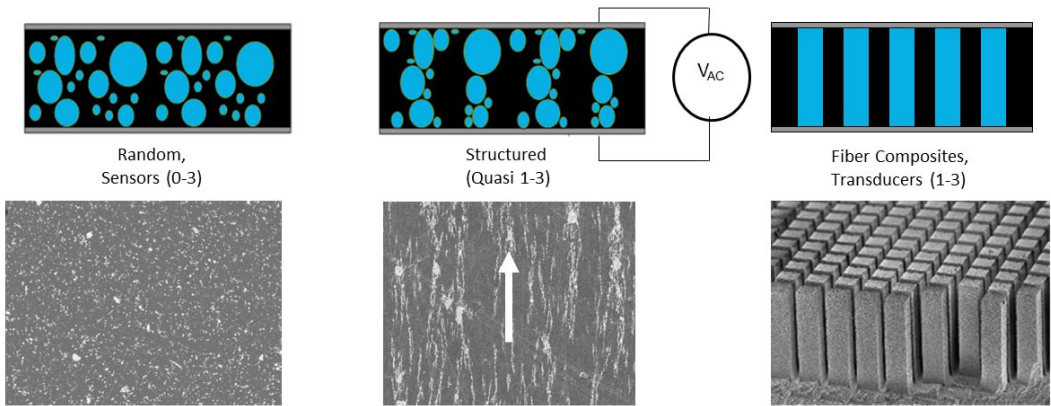


Figure 8. Graphical representation of 0-3, quasi 1-3 and conventional ceramic pillars 1-3 composite types along with their corresponding SEM micrographs; in random and quasi composite, the polymer matrix is white whilst ceramic filler is grey coloured from [34] and [106].

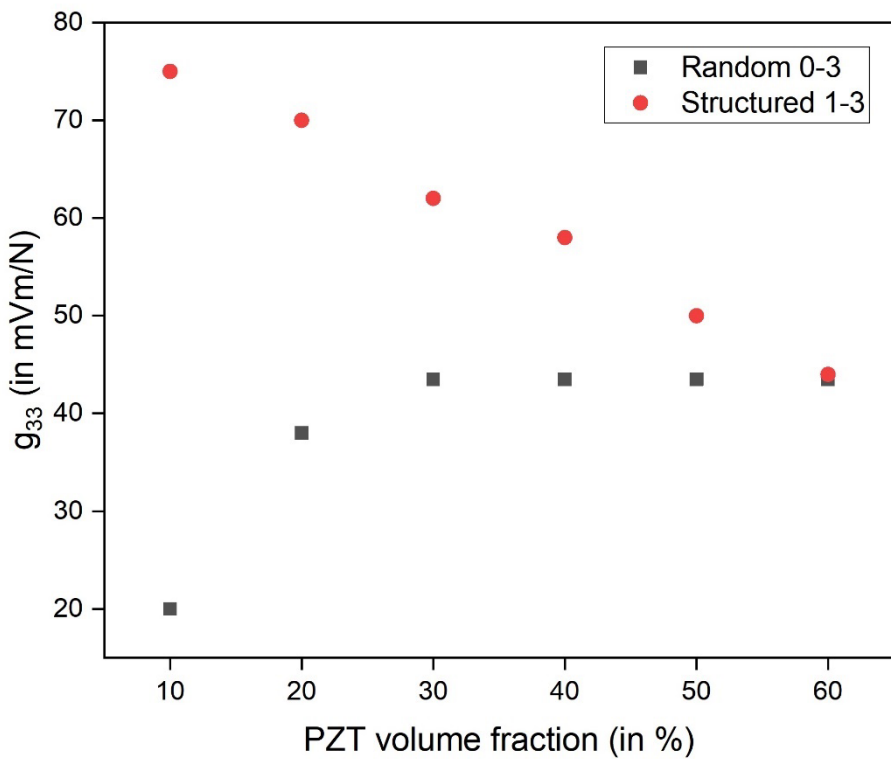


Figure 9.  $g_{33}$  of random 0-3 and structured (quasi) 1-3 PZT/polymer composite at various PZT volume fraction adopted from [129]

## List of Tables

Table 1. Summary of temperature dependence of dielectric constant for various volume fraction of BT in PVDF/BT composites at 100kHz <sup>a</sup> .....	55
Table 2. Summary of mean remnant polarisation and saturation polarisation of 1-3 piezocomposite as a function of filler fraction volume [91]. .....	56

Table 1. Summary of temperature dependence of dielectric constant for various volume fraction of BT in PVDF/BT composites at 100kHz<sup>a</sup>.

BT filling content (volume Fraction) %	Operational Temperatures			
	-50°C	10°C	90°C	130°C
	Dielectric Constant			
0	6	8	12	12
20	12	20	25	25
60	60	88	110	110
80	50	73	77	80

<sup>a</sup> Source of results: Fu et al. [84]

Table 2. Summary of mean remnant polarisation and saturation polarisation of 1-3 piezocomposite as a function of filler fraction volume [91].

Fibre (PZT) volume fraction (%)	Remnant polarization (c/m <sup>2</sup> )		Mean Remnant polarization (c/m <sup>2</sup> )	Saturation polarization (c/m <sup>2</sup> )		Mean Saturation polarisation (c/m <sup>2</sup> )
	Expt.	Theoretical		Expt.	Theoretical	
35	0.1	0.1	0.1	0.11	0.1	0.1
65	0.23	0.2	0.22	0.27	0.25	0.26
80	0.28	0.28	0.28	0.35	0.34	0.35
100	0.35	0.36	0.36	0.39	0.37	0.38